Master Thesis in Geographical Information Science nr 157

Urban tree canopy mapping -an open source deep learning approach

Tobias Rydlinge

2023

Department of

Physical Geography and Ecosystem Science

Centre for Geographical Information Systems

Lund University
Sölvegatan 12

Tobias Rydlinge (2023). Urban tree canopy mapping -an open source deep learning approach
Master's degree thesis, 30 ECTS credits in Master in Geographical Information Science
Department of Physical Geography and Ecosystem Science, Lund University

Supervisor: Abdulhakim Abdi, Researcher, Centre for Environmental and Climate Science, Lund university

Preface

I work as a GIS-engineer in Borås and as a consultant within the field of remote sensing.

My background with parents working as gardeners in a family firm and with a MSc in Biology mapping trees has always been something that interested me. Mapping and measuring nature have always caught my interest. All kinds of automation, coding, the fascination of trying new remote sensing techniques and maybe the laziness of doing manual work led me to machine learning.

I would like to thank my supervisor Abdulhakim Abdi, Researcher, Centre for Environmental and Climate Science, Lund University for valuable feedback.

Most of all want to thank my wife and my three sons for their support and patience with me working on my thesis. Working full time with children and studying has been a tough challenge.

Urban tree canopy mapping - An open source deep learning approach

Abstract

Urban trees have an important role to provide ecosystem services and to make our cities greener and more sustainable. The changing climate and densification of cities make it even more valuable to preserve and investigate in urban trees. Tree canopy detection in cities is challenging, with both trees and other objects of irregular shape, size and complexity. The aerial images from Lantmäteriet (the Swedish mapping cadastral and land registration authority) is a great source for image analysis on high resolution images, but the leaf-off images may be challenging for tree canopy detection.

The aim of the study was to test if Light Detection and Ranging (LIDAR) could be combined with aerial images to develop a deep learning tool for urban tree canopy mapping under leaf-off conditions. The deep learning method using LIDAR and aerial leaf-off images had a precision of 88 % mapping urban tree canopy. Using the same method with LIDAR and IR leaf-on data yielded a precision of 91 %. The LIDAR data increases the accuracy for leaf-off data when added to the deep learning model.

The findings of this study indicate that tree canopy mapping with LIDAR and aerial images taken under leaf-off conditions can be used for tree canopy mapping with comparable results to other methods.

KEYWORDS: Machine learning, deep learning, urban tree canopy, remote sensing

Table of contents

List of Abbreviations

CHM	Canopy Height Model
IR	Infrared
LIDAR	Light Detection and Ranging
ResNet	Residual network
RGB	Red Green Blue

List of Tables

List of Equations

List of Figures

1. Introduction

1.1 Ecosystem services provided by urban trees

Urban forestry is the sustained planning, planting, protection, maintenance, and care of trees, forests, greenspace in cities and communities for economic, environmental, social, and public health benefits for people (Deneke, 1993).

City planning is facing a huge paradigm shift in terms of how we look at urban spaces and urban greenery. The Covid-19 pandemic has made us revaluate on how we use our nearby public green spaces. Due to urban densification green spaces are increasingly important for the human wellbeing and health. The value of urban green spaces has been studied more intense the last years and green infrastructure and urban green spaces are topics on the nature based solutions agenda for both stakeholders and city planners (de la Barrera et al., 2023).

There are many motives of doing a deep learning based urban tree mapping on city level. The analysis is relatively easy to perform and can be updated regularly with data from Lantmäteriet (the Swedish mapping cadastral and land registration authority). Another advantage is that data, method and competence will be owned by the municipality itself. Officers working with tree planning are in need of tools when communicating with local politicians and stakeholders. Deep learning and remote sensing can help us make data driven decisions on updated data. Where do we need to plant new trees? Where are the empty spots? Does citizen inequity regarding nearby green spaces exists? As cities densifies the pressure on urban green spaces increases and strategic urban green space management may compensate for the land use change (Balikçi et al., 2022). Detailed and updated data also facilitates a cost effective maintenance of urban trees, e.g. by maintaining coherent tree structures (A. Spets, city gardener, Borås stad, personal communication, January 31, 2023).

Storm water management in cities face several challenges because of climate change and inefficient urban drainage systems (Prudencio and Null, 2018). Urban heat islands, characterised by higher temperatures in densely built-up areas (Oke, 1982) is another contemporary problem in cities. Urban trees can help with evaporation, as shading from leaves provides a cooling effect, where solar radiation otherwise would hit direct on a surface, is blocked from reaching the surface below (Hayes et al., 2022). Environmental noise exposure is a global public health concern, with implications for physical health, wellbeing, and mortality. Globally, traffic noise is a major source of environmental pollution (Karimi et al., 2010), and it is estimated that one million healthy life years are lost every year to traffic related noise in the western part of Europe (Khreis et al., 2016). Vegetation, in particular trees, can have a substantial impact on the level of traffic noise experienced by residential properties (Van Renterghem, 2014). Trees facilitate noise reduction through two main mechanisms: The absorption of sound energy by soft green vegetation, and the redirection and scattering of sound waves by woody structures e.g., trunks, branches and stems (Fletcher et al., 2022). Urban trees can also improve mental health. A canopy cover of 30 percent has a proven effect (Astell-Burt and Feng, 2019) on mental health and has therefore

become an international guideline for the global work with urban green spaces (Bosch, 2021).

1.2 Machine learning and deep learning

Data science is an interdisciplinary field focused on extracting knowledge from data sets. Machine learning is a subfield of artificial intelligence, which can be defined as the capability of a machine to imitate human behaviour. Artificial intelligence is used to perform tasks in a way similar to humans (Choi et al., 2020). Machine learning is used to get computers to act without being programmed and has helped us to develop self-driving cars, speech recognition and effective web search. Deep learning is a subset of machine learning

(Figure 1). A deep learning algorithm is reiterating and performing a task repeatedly and improving for every iteration, in order to improve the result. Artificial neural networks are inspired by the human brain.

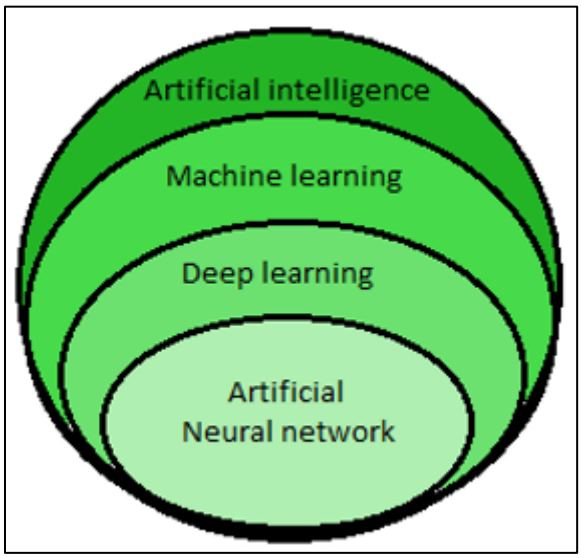

Figure 1. Artificial neural networks used in deep learning are subfields of artificial intelligence. Image by author

Neural network architectures are the most frequent deep learning methods, and that is why deep learning models often are called deep neural networks. Traditional neural networks has 2-3 hidden layers but deep networks can have as many as 150. Large sets of labelled data are used as training material for neural network architectures as they learn features from the data. Artificial neural networks are comprised of a node layers, containing an input layer, one or more hidden layers, and an output layer (Figure 2) (Pyo et al., 2017). Each node connects to another. The input layer is responsible for accepting the inputs, the hidden layer processes the input data to find out hidden information and performs feature extraction, and the output layer gives the desired output. ("What is Deep Learning? | IBM," 2020).

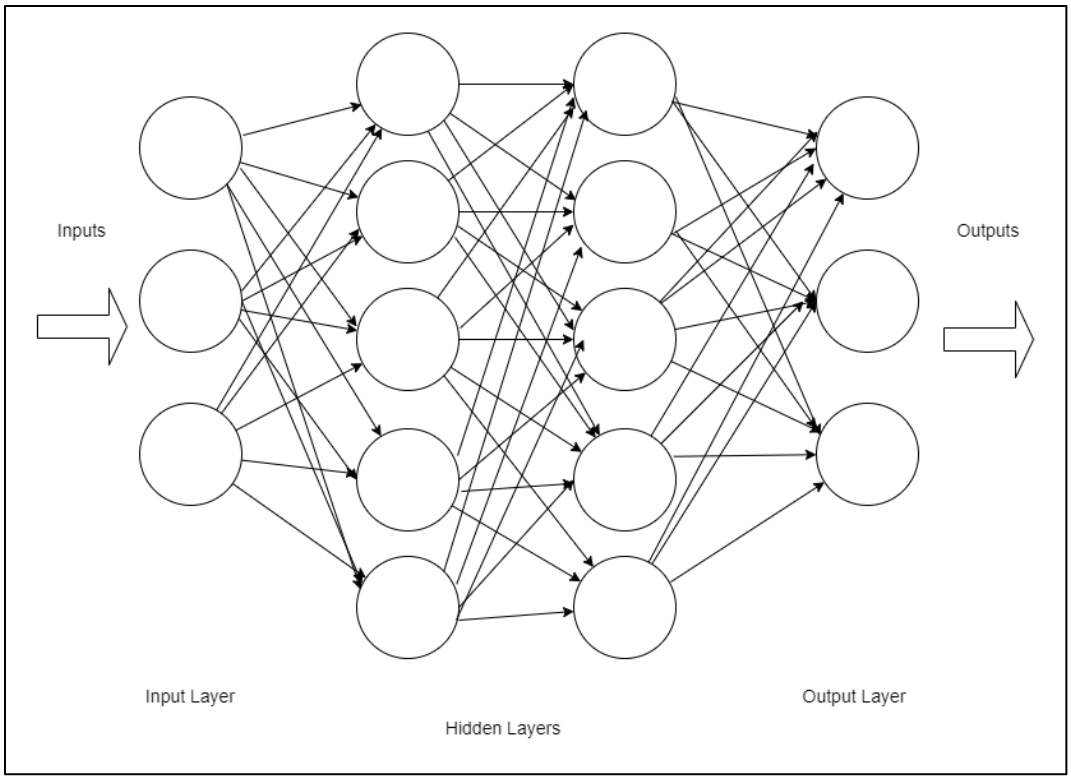

Figure 2. Neural network with input layer, hidden layers and output layer. Inputs are training data and outputs are prediction results. Image by author.

Raster Vision, the python framework used for this study, is using a DeepLabV3 model with a ResNet-50 backbone. ResNet stands for Residual Network and is a specific type of convolutional neural network with 50 layers (He et al., 2016). The important difference from a normal neural network is the residual block using skip connections. The skip connections preserve information without adding much of overload on the network from initial layers until the last. Residual networks seems easier to optimize than traditional neural networks (He et al., 2016). The main benefit of the residual network architecture is how it performs in training errors affecting the model accuracy.

The ResNet-50 model architecture (Figure 3) starts with Zero padding, a technique that preserves the original input size of the image. The Rectified Linear Unit (ReLU) activation function is a function that will output the input directly if it is positive, otherwise, it will output zero. Maximum pooling is a pooling operation that calculates the maximum value in each patch. Average pooling is calculating the average for each patch. Convolutional layers are the main building blocks in convolutional neural networks. (“A Gentle Introduction to Pooling Layers for Convolutional Neural Networks - MachineLearningMastery.com,” 2023) Flattening converts the data into a single long continuous linear vector and the fully connected (FC) layer adds the output.(“Convolutional Neural Network Tutorial [Update],” 2023)

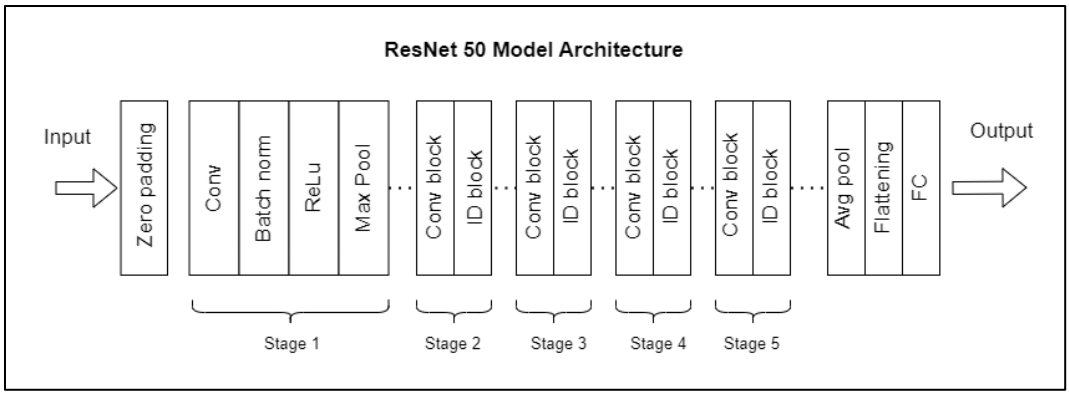

Figure 3. The ResNet-50 model architecture. Image by author.

The models, loss functions, and optimizers for Raster vision are based on PyTorch and are configurable, e.g. batch size and number of epochs can be set in the code. Augmentors used in this study were the default augmentors RandomRotate90, HorizontalFlip and VerticalFlip.

Raster vision is using cross entropy loss as default loss function , which computes the loss between true labels and predicted labels ("Probabilistic losses," 2023). Use this cross-entropy loss for binary (0 or 1) classification applications. The training loss is a metric used to assess how a deep learning model fits the training data. Loss is a number indicating how incorrect the prediction was on a single example. If the prediction is perfect, the loss is zero ("Descending into ML: Training and Loss | Machine Learning Crash Course | Google Developers," 2022).

1.3 Mapping urban trees

1.3.1 Technique and challenges in mapping urban trees

Manual assessment of aerial images was a common method in the beginning of the remote sensing history in the forestry industry and for land-cover mapping (Heller, 1964). Tree canopy cover is traditionally measured using vegetation indices, e. g. normalized difference vegetation index (NDVI) (Rouse et al., 1973) using satellite imagery to measure the amount of green vegetation. Infrared (IR) images can also be used to analyse vegetation (With and With, 2019). Classification can be made by pixel based classification (Richards and Jia, 1999), using the spectral information available for an individual pixel or object based classification (Blaschke et al., 2014), which analyses the spatial properties of each pixel and how they relate to other pixels. Pixel based classification methods have their drawbacks because they rely on spectral signatures of individual pixels (Myint et al., 2011). The object based approach (OBIA) relies on the expert experience and local knowledge in the process of determining the most appropriate scales, parameters, functions, and classifiers. As a result, OBIA classification results may vary widely from case to case and from person to person (Wang et al., 2021). There has been a significant increase in popularity among land cover classification studies recent years (Abdi, 2020) and deep learning is gaining more attention in the field of image recognition due to faster computers, better algorithms and more easy

accessible frameworks and open source solutions . Deep learning minimizes the human interaction and expertise in the classification process results and can be used with different data sources, e.g. LIDAR, NVDI and RGB images. The convolutional neural network, in particular, has been successfully applied in object detection and semantic segmentation (Ondruska et al., 2016; Qian et al., 2015) and also used in urban tree mapping with highly accurate results (Timilsina et al., 2020). Individual tree species mapping of 8 species, using deep learning was done in St. Louis, USA, with an accuracy of 82.4 % using LIDAR and satellite images (Hartling et al., 2019). Another study used similar data to map urban tree cover in 34 Chinese cities (Pu and Landry, 2020).

Lantmäteriet (the Swedish mapping cadastral and land registration authority) provides aerial images within the national acquisition programme. However, imagery for detailed measurement of urban areas for municipal detailed planning and documentation, good visibility towards the ground must be sought. The most suitable period is in the spring between snowmelt and leafing (Lantmäteriet, 2017). The aerial images from Lantmäteriet are a great source for image analysis on high resolution images, but the leaf-off images may be challenging for tree canopy detection. One drawback is the deficiency of IR-information before leafing, meaning that IR cannot be used in the analysis. However aerial images still remain very interesting if they can be used for tree canopy mapping. Adding LIDAR data is also be highly interesting as it may compensate for the leaf-off status by adding data input to the machine learning model. The elevation data is one parameter to delineate trees from their surroundings.

1.4 Research problem and objectives

Tree detection in cities is challenging, given the irregular shape, size, occlusion, and complexity of urban areas (J. A. C. Martins et al., 2021). Open datasets e.g. LANDSAT, are still not detailed enough for urban tree crown mapping. The challenge in mapping urban trees for the scientific community is to create generalizable, replicable, and powerful models that allow the use of multiple data sources for urban forest inventory automation (Lin et al., 2019; Vauhkonen et al., 2014). It´s also crucial to solve problems with different spatial and temporal resolution from different data sources (Ma et al., 2019). Thus, this study addresses the problem and test aerial images before leafing can be used for tree canopy detection with the combination of LIDAR data.

This study aims to answer the following research question:

Q1: Can Light Detection and Ranging (LIDAR) be combined with aerial images to develop a deep learning tool for urban tree canopy mapping under leaf-off conditions?

Q1 will be addressed through the following objectives:

1. Evaluation of the prediction accuracy with validation metrics.
2. Identification of strengths and weaknesses in the deep learning model through detailed examination of different categories of predictions.

2 Methods

2.1 Study area

The study area (Figure 4) is the urban area of Borås in the county of Västra Götaland in the southwest of Sweden. The city of Borås is situated 155 meters above sea level and the mean annual temperature and precipitation is 7.6 C and 1008 mm respectively (Fick and Hijmans, 2017). The most common tree species in the urban part of Borås are European white birch (Betula pendula) 21.3%, English Oak (Quercus robur) 10.5% and Norway spruce (Picea abies) 8.4%, according to an i-tree inventory ("i-Tree Eco Field Guide 4.26.2016," 2016) conducted 2019 at 200 randomly selected spots.

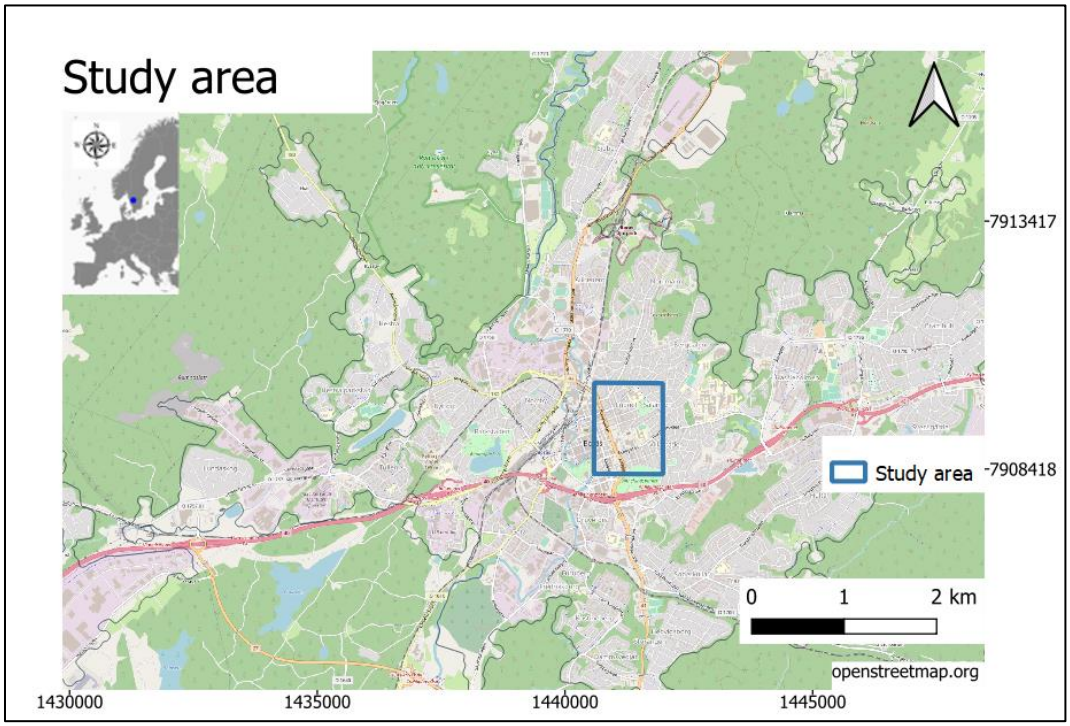

Figure 4. The study area marked with blue outline.

2.2 Methodological overview

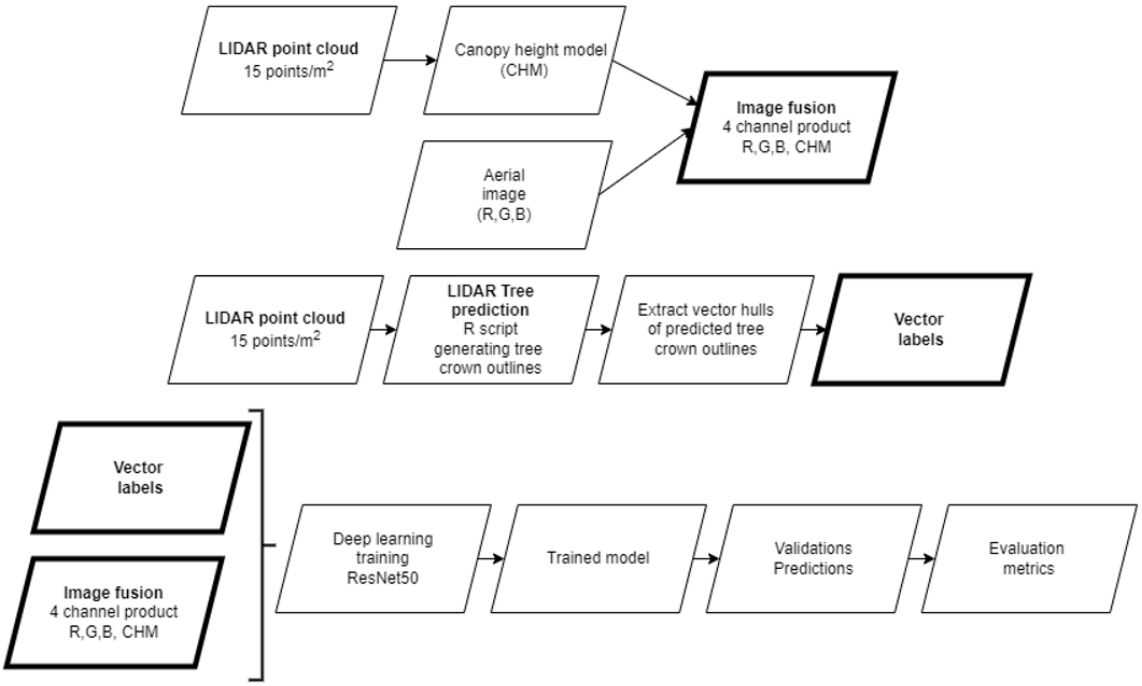

Figure 5. Flowchart describing the method of tree canopy extraction.

Figure 5 illustrates the process of urban canopy mapping. It is a linear process from LIDAR point cloud and aerial images to a final prediction model for urban tree canopy classification. The first step is to make a canopy height model (CHM) from LIDAR data. The CHM is then merged with an aerial image to create an image with 4 bands. The LIDAR point cloud is also used to extract labels of tree canopies using watershed image segmentation. Vectorised labels are combined with the 4-band image in the training phase of the deep learning model. The trained model is used for prediction of tree canopy on new images and the results pixel-based prediction are evaluated with accuracy metrics.

2.3 Creating image input for deep learning model

A canopy height model (CHM) is an elevation raster with the height of trees, buildings, and other structures above the ground topography. A CHM is made from LIDAR data.

2.3.1 Light Detection and Ranging (LIDAR data)

LIDAR data are 3D measurements of light reflections from the ground, vegetation, and other objects collected from an aircraft. The coordinate measurements are based on the laser pulses combined with sensor position from Global Navigation Satellite Systems (Figure 6) (Ressl et al., 2009).

A LIDAR scanning for Borås municipality was done in November 2016. The result from the LIDAR scanning was a point cloud with an average of 15 points per square meter, with values for x, y and z coordinates. The result was delivered in 500*500m tiles with data.

The LIDAR point cloud was delivered classified for ground and buildings (ASPRS - American Society for Photogrammetry & Remote Sensing, 2002). Vegetation was not classified.

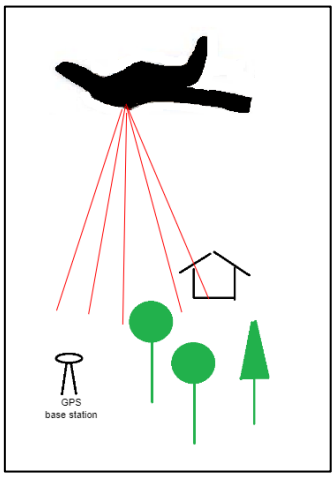

Figure 6. Airborne LIDAR-scanning. Image by author.

The process to create the CHM was done with the following steps:

1. The ground points were normalized to 0 elevation, instead of meters above sea level. The height was set relative to closest ground height points. This was done because the deep learning model should identify trees correctly based on their absolute height and not based on the height, they stand above sea level.

2. Outliers were removed with a filter function. Points above 95th percentile of height were removed. The LIDAR data may contain noise, therefore this was done.

3. Null values (missing data) were removed to create a pit free CHM (Khosravipour et al., 2014). This was done to get a smoother final product.

4. The results were saved as a 32 centimetres resolution CHM.

2.3.2 Image data

The image data used in the thesis was aerial images, IR-image and CHM (Table 1). The aerial images were captured at 3700 meters above ground with a digital camera, UltraCam Eagle Mark 3. The aerial image had 3 bands (red, green and blue) and covered the study area (Figure 4). The digital aerial images had a resolution of 16 centimetres. The aerial image was cut out at same size as the CHM. The result was an aerial image tile at the same size as the CHM raster.

Table 1. Raster data used for different band set ups.

Imagery	**Resolution**	**Acquisition date**	**Foliage**	**Data type**
Ortho imagery, 3 band (R,G,B)	16 cm	2020-04-20	Leaf-off	Integer 32
Ortho imagery, 3 band (R,G,B)	16 cm	2022-06-18	Leaf-on	Integer 32
Ortho imagery, 3 band (IR,G,B)	16 cm	2022-06-18	Leaf-on	Integer 32
Canopy height model (CHM)	32 cm	2016-11-24	Leaf-off	Floating

Image input used to train the different models Figure 7- Figure 10 show the different images over the training area.

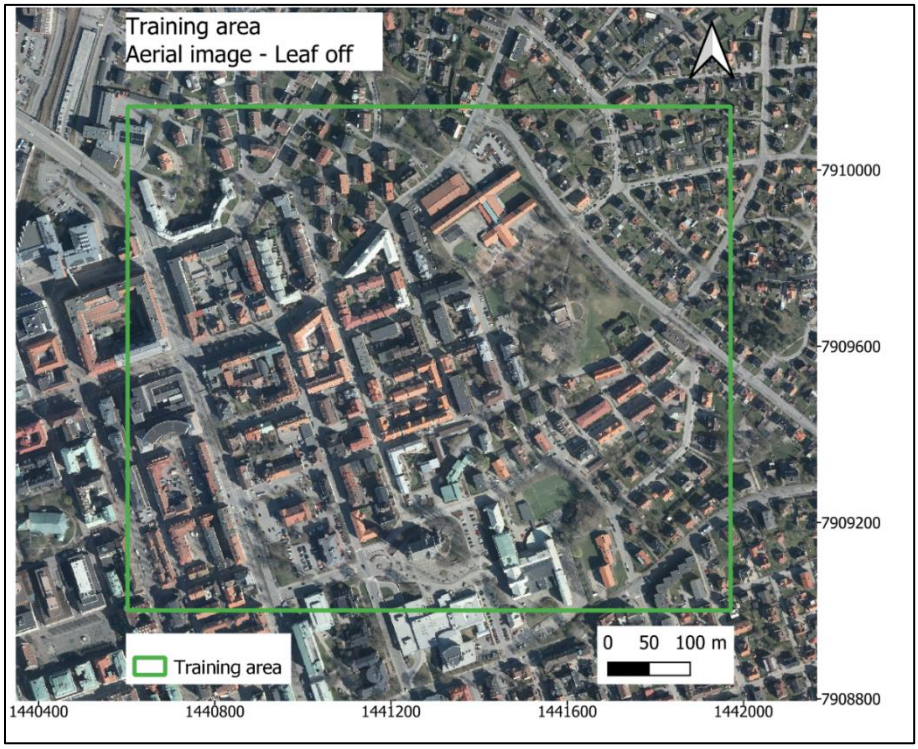

Figure 7. Leaf-off imagery from 2020-04-20, Lantmäteriet. Training area marked with green outline

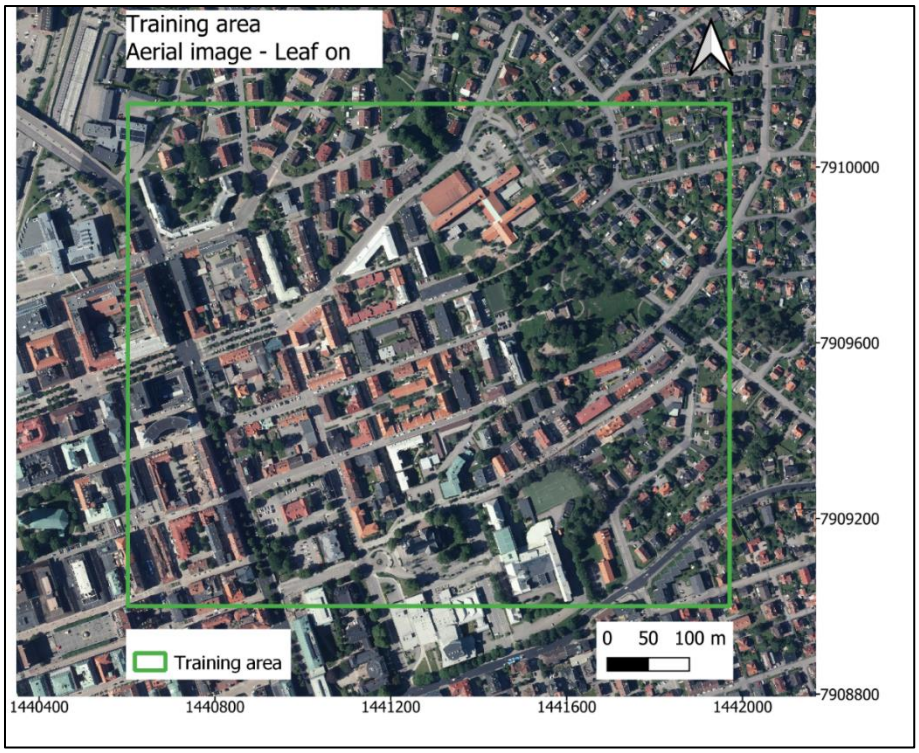

Figure 8. Leaf-on imagery from 2022-06-28, Lantmäteriet. Training area marked with green outline.

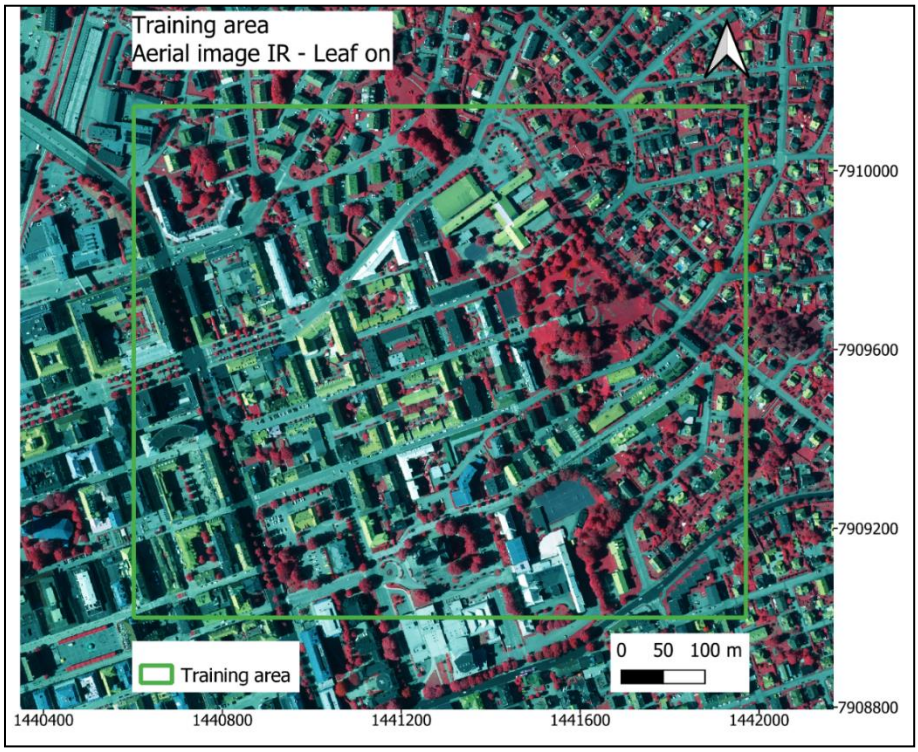

Figure 9. Leaf-on infrared (IR) imagery from 2022-06-28, Lantmäteriet. Training area marked with green outline.

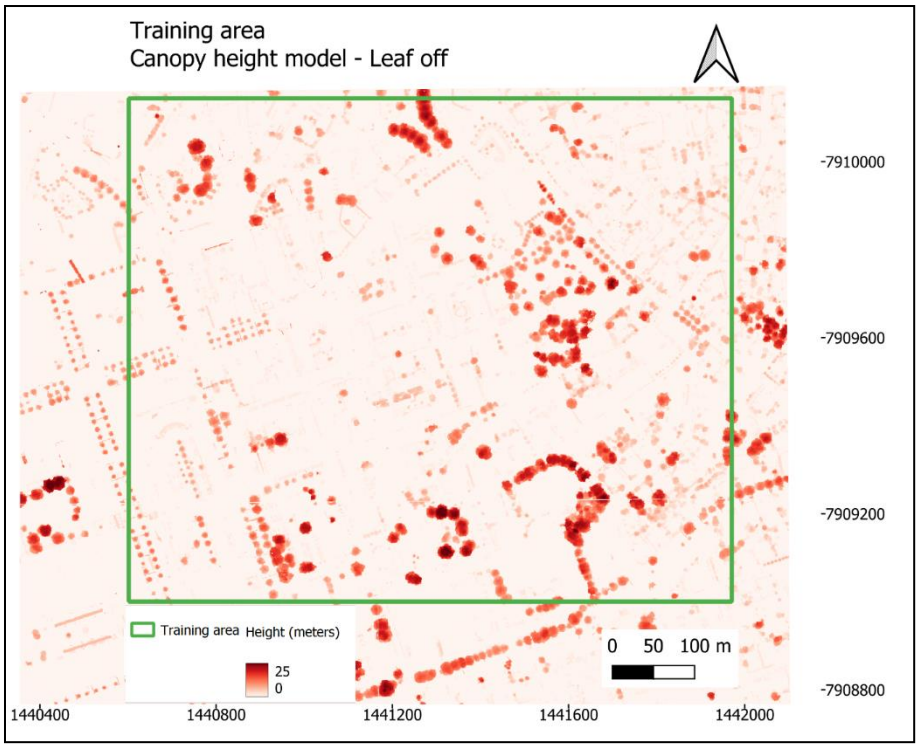

Figure 10. Canopy height model made from LIDAR ground points and unclassified point cloud data (buildings not included), 32 cm resolution. Elevation relative to ground level.

Different raster band combinations (Table 2) were tested to analyse the difference in prediction accuracy with different types of image input.

Table 2. Raster image band combinations as input for model training.

Band set-up	Foliage
IR,G,B+CHM	Leaf-on
R,G,B + CHM	Leaf-on
R,G,B	Leaf-on
R,G,B + CHM	Leaf-off
IR,G,B	Leaf-on
R,G,B	Leaf-off
CHM	Leaf-off

2.3.3 Image fusion

For some of the band combination a 4th band was added (Figure 11). In those cases, the CMH (1 band) was merged with the aerial image (3 bands). The result was a 4-band image with 32 centimetres resolution.

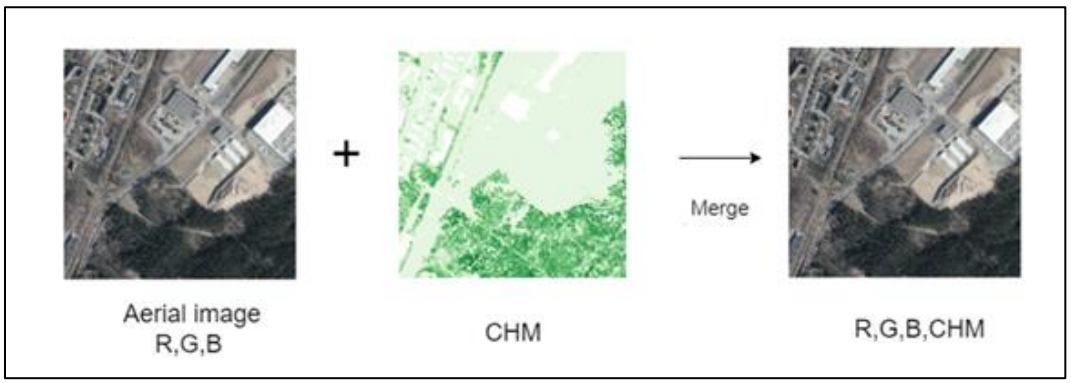

Figure 11. Example of fusion done with canopy height model and aerial image. The result was a 4 band image.

2.3.4 Watershed segmentation

The tree segmentation using a CHM is based on the assumption that each tree has a treetop representing a local maxima regarding the elevation. The height values of the CHM have local maxima and minima values, those can be referred as watersheds and basins (Figure 12).

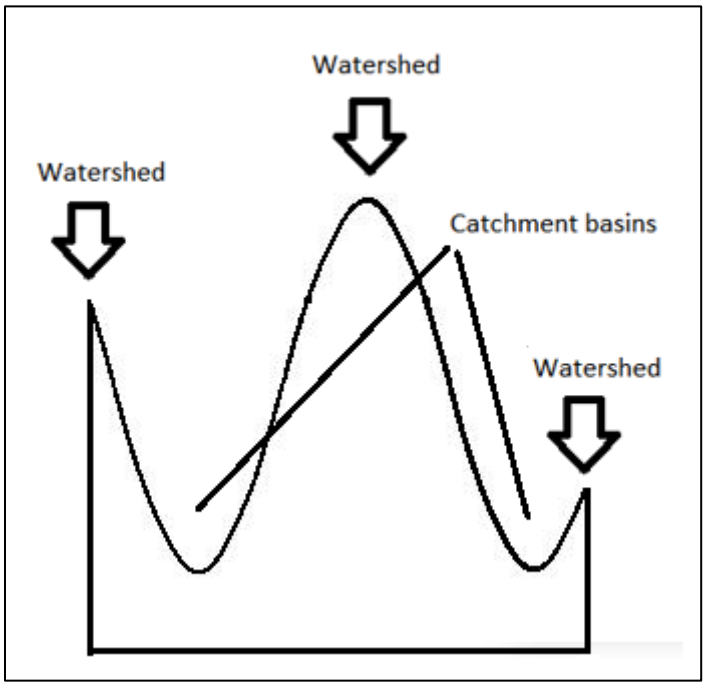

Figure 12. Illustration of the concept of watershed segmentation. Height profile of CHM, catchment basins and watersheds. Image by author.

The watershed algorithm identifies and separates image objects that stand out of the background (Oleś et al., 2020). The pixels are classified as canopy or ground pixels with 4 meters as a separation between canopy and ground hits.

The algorithm searches neighbouring pixels to decide whether the pixels are within a tree crown or outside. If neighbouring pixels are canopy pixels, the central pixel will be classified as a within the crown. All tree crown pixels in the image will be assigned the ID number of the associated watershed.

The first step to get training data was to use a script conducting the watershed algorithm to generate tree hulls automatically (Figure 13) running a script in R (a free software environment for statistical computing and graphics). This speeded up the process substantially since creating training samples for machine learning is considered to be a time consuming task ("Data Preparation in Machine Learning: 6 Key Steps," 2023)

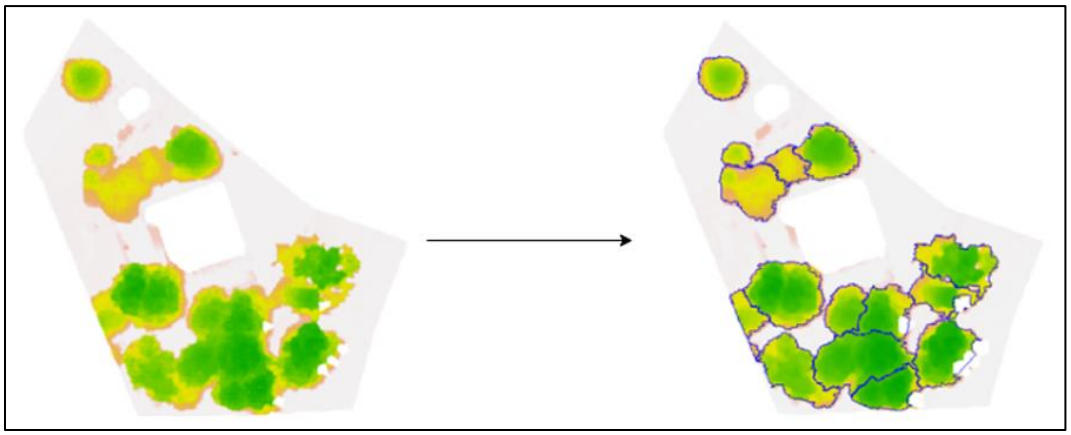

Figure 13. Tree labels from CHM with the watershed algorithm using R.

A manual revision was done using the latest images, IR and CHM after the automatic delineation. The manual work was done to guarantee the best quality of the training and validation samples.

2.3.5 Setting up the machine learning framework

Image data with marked annotations of trees (labels) were used as input (Figure 14) to the machine learning model. Feeding the model with raster data of trees of different size and shape will train the deep learning model to detect trees on new images. This is the core function of deep learning on image data.

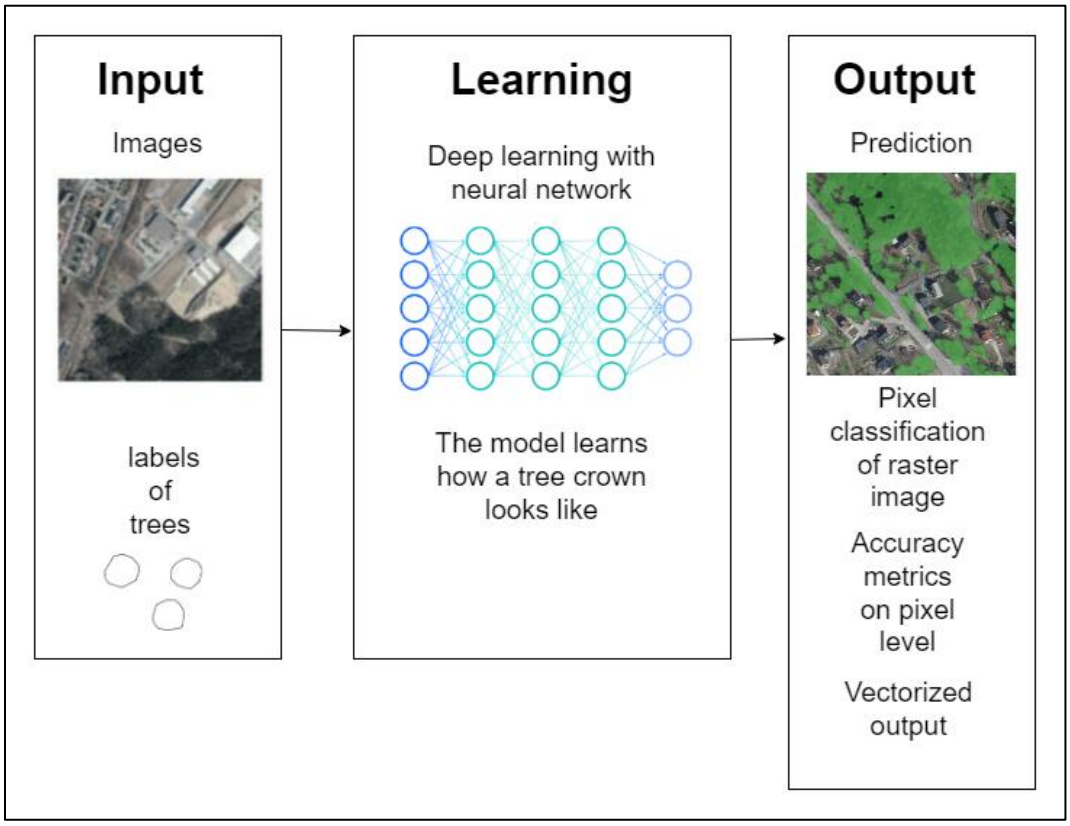

Figure 14. Data input, deep learning with neural network and output.

The software used for the deep learning training was Raster Vision version 0.20.
Raster Vision is an open source framework to build deep learning models on satellite, aerial, or drone images. An open source framework is a template for software development that is designed by a social network of software developers, e.g. github (https://github.com/azavea/raster-vision) as in this case. These frameworks are free for public use and provide the foundation for building a software application. There is built-in support for object detection and semantic segmentation using python code (programming language). Object detection means predicting a bounding box enclosing the object of interest while semantic segmentation assigns a label to each pixel in an image. Since tree canopy area was interesting in this study semantic classification was used.
The software was installed in a Docker environment. The reason for that is that the python dependencies are much easier to handle in a Docker container rather than in a local environment. Docker is an open source containerization platform. It enables to package applications into isolated development environments called containers ("What are containers? | Google Cloud," 20230131). The input to a Raster Vision is a set of images and

training data. The output of a Raster Vision is a trained deep learning model that allows prediction on new images.

The model was trained with 10 epochs (the epochs are the number of passes of the entire training dataset the machine learning algorithm has completed.) on a 32 GB RAM, Intel Core i7 processors, PC Workstation. Each epoch took approximately 15 minutes.

Training and validation was performed on the same data, e.g. data trained on leaf-on and CHM was validated on leaf-on and CHM raster. The validation labels however were the same for all models.

2.3.6 Evaluation metrics

2.3.6.1 Precision

Precision is true positives (tp) devided by true positives (tp) and false positives (fp) (Equation 1) (Witten and Frank, 2023). Precision is an interesting measure telling us about how the true negatives and how they affect the accuracy.

$$\text{precision} = \frac{\text{tp}}{\text{tp} + \text{fp}}$$

Equation 1. Derivation of the precision. True positive (tp), false negative (fn) and false positive (fp).

2.3.6.2 F1 Score

F_1 score is widely used for machine learning accuracy tests (Equation 2). That is why it was chosen as evaluation metrics for the precision of the tree canopy classification. The F1-score, is a measure of the accuracy on a dataset. Recall represents the ability to correctly predict the positives out of actual positives. Recall is the number of true positives divided by the number of true positives and the number of false negatives. Precision, or positive predictive value, is the proportion of true positives out of the total number of positive predictions. The range of F1 is between 0 and 1, with 0 being the worst score and 1 the best score (Tao et al., 2021). The F1-score is described by equation 1. The metrics is based on how each pixel in the images is classified, tree or background in this case.

$$F_1 = \frac{2}{\text{recall}^{-1} + \text{precision}^{-1}} = 2 \cdot \frac{\text{precision} \cdot \text{recall}}{\text{precision} + \text{recall}} = \frac{\text{tp}}{\text{tp} + \frac{1}{2}(\text{fp} + \text{fn})}.$$

Equation 2. Derivation of the F1 score. True positive (tp), false negative (fn) and false positive (fp).

2.3.7 Training and validation area

The training area (Figure 15) is situated in the city centre of Borås. The area has both single tree stands and denser areas of tree stands, in particular in the western part of the area. The training area is representative for a city centre with high-rise buildings (3-12 floors) in blocks. The training area contained 1103 vector labels of tree canopies used as training data. The validation area (Figure 15) contains the heterogeneity regarding size, colour and shape of tree canopies that can be found in the training area, both single trees and dense tree stands of tree canopies were used as validation data.

The area is the central southern part of the dense city centre, mainly higher buildings, some open impervious areas and tree avenues with older trees are primary characteristics of the validation area. The validation area contained 616 vector labels used as validation data for the test of F1-score accuracy.

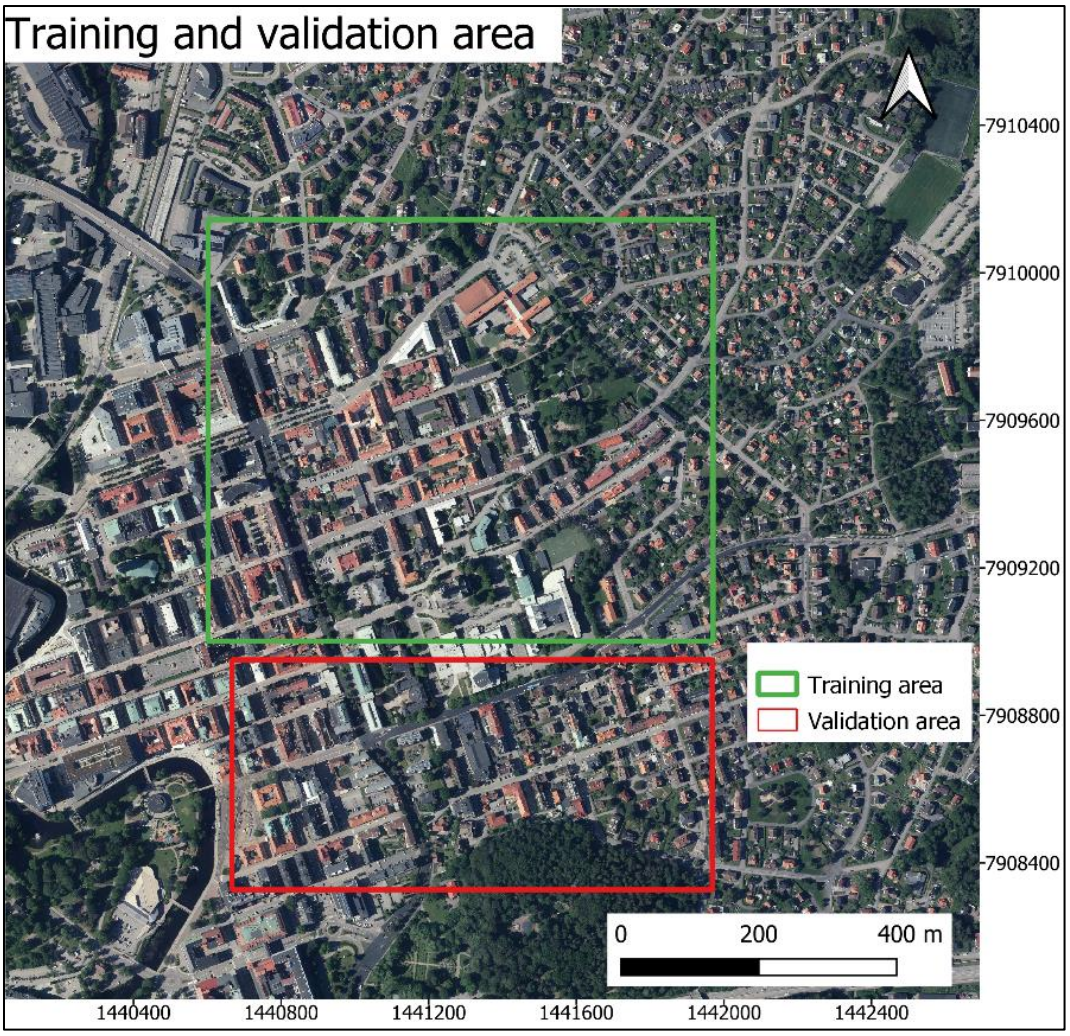

Figure 15. Training area, 45 ha, marked with green outline and validation area, 23 ha, marked with red outline.

3 Results

7 different set-ups for band combinations (Table 3) were tested for F1-score and precision. True positive (TP), false negative (FN), false positive (FP) and true negative (TN) was automatically calculated in the Raster vision pipeline output. The results was put in a confusion matrix. The band setup IR,G,B,CHM scored the highest total accuracy. Leaf-on imagery was used in the three top predictions while R,G,B,CHM was similar of using leaf-on imagery only. IR,G,B,CHM scored the highest accuracy.

Table 3. Confusion matrix, pixel level statistics, table shows percentage of all pixels in validation image.

Band set-up	Foliage	TP	TN	FP	FN	F1 score	precision
IR,G,B,CHM	Leaf-on	14.39%	82.42%	1.38%	1.81%	0.89	0.91
R,G,B, CHM	Leaf-on	14.32%	82.91%	1.50%	1.37%	0.88	0.91
R,G,B	Leaf-on	13.43%	82.90%	1.51%	2.16%	0.87	0.90
R,G,B, CHM	Leaf-off	13.50%	82.31%	1.83%	2.10%	0.87	0.88
IR,G,B	Leaf-on	13.18%	82.22%	1.58%	3.02%	0.79	0.88
R,G,B	Leaf-off	9.72%	82.53%	1.87%	5.88%	0.68	0.84
CHM	Leaf-off	12.32%	82.31%	2.10%	3.27%	0.68	0.83

Figure 16 - Figure 19 show the predictions of tree crowns within the validation area for the 4 prediction models that scored highest accuracy. Most predictions are similar for all 4 models, however there are some important diffences, e.g. how single trees are detected. All models are underestimating the overall tree area and the number of trees in the the validation area.

Figure 16. Validation area with tree predictions by model trained on leaf-off and CHM imagery.

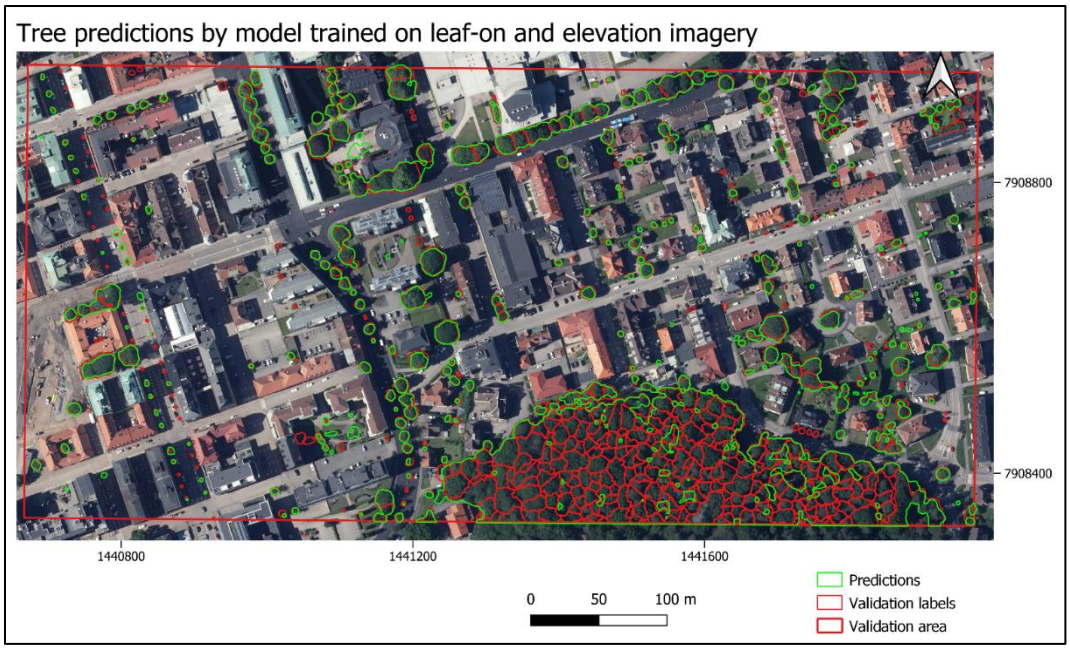

Figure 17. Validation area with tree predictions by model trained on leaf-on and CHM imagery.

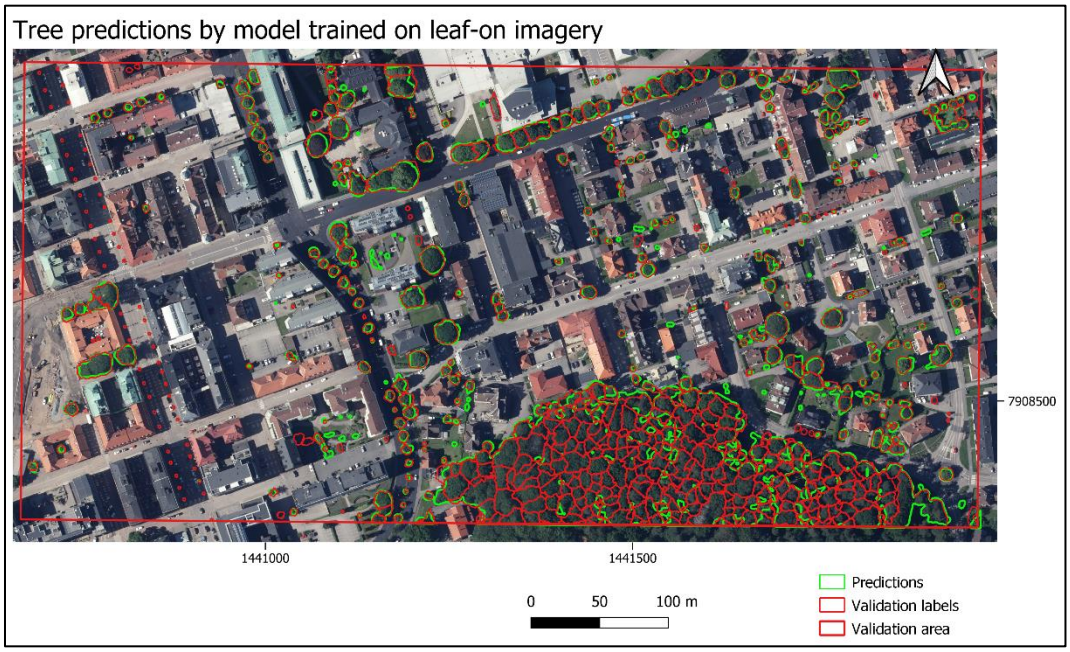

Figure 18. Validation area with tree predictions by model trained on leaf-on imagery.

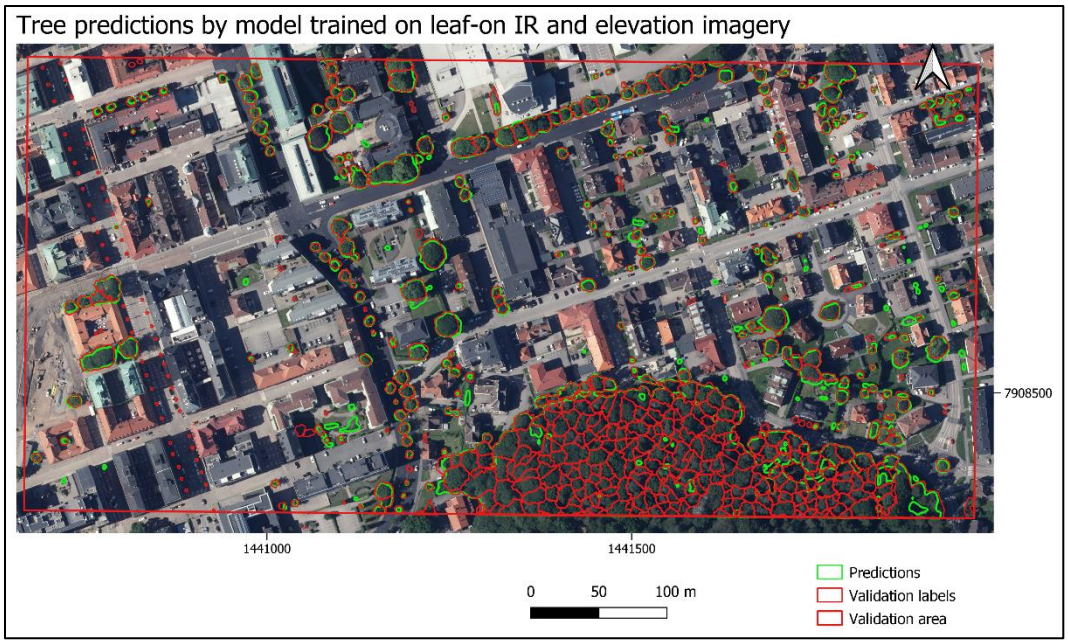

Figure 19. Validation area with tree predictions by model trained on leaf-on IR and CHM imagery.

3.1 Prediction details

The avenue of trees (Figure 20) with small crowns shows great differences between the 4 models. The R,G,B leaf-on model has most problem detecting the crowns. The leaf of model (R,G,B, CHM) is overestimating the crown area. The model using leaf-on with IR and CHM (IR,G,B,CHM) only spots 2 trees in the avenue. Leaf-on CHM (R,G,B,CHM) gives the best result with less overestimation of tree crown area. Only RGB leaf-on data does not detect a single tree while the model with CHM added detects 7 trees (Figure 20).

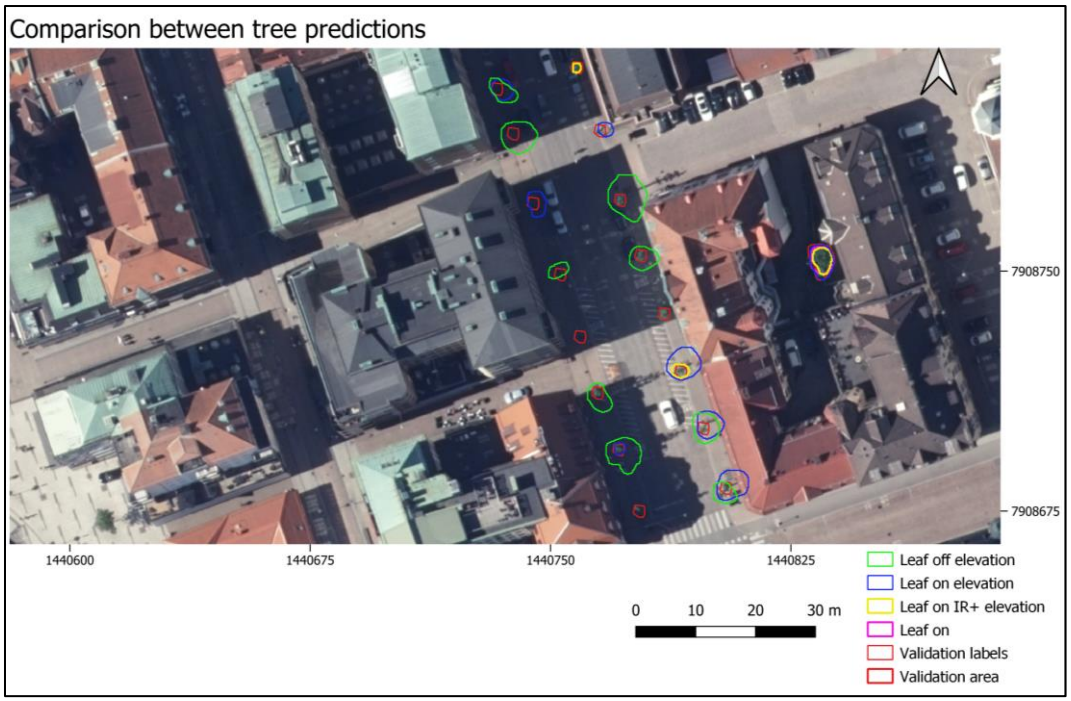

Figure 20. Avenue of trees with small crowns predicted by different model setups.

Large dense tree crowns in a row (Figure 21) are detected similar by all 4 models. Some differences can be seen for single tree predictions where leaf-on with IR and CHM is most correct with validation labels.

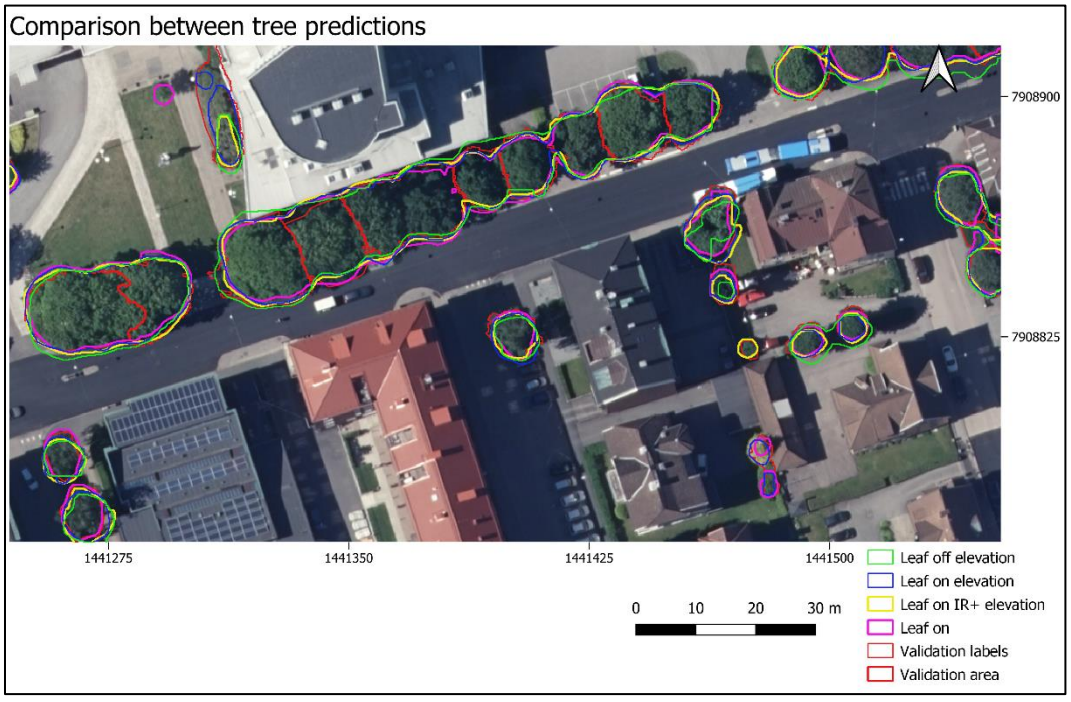

Figure 21. Row of trees with dense crowns and single trees predicted by different model setups.

The metal rails holding road signs in seems like an issue (Figure 22) for the leaf-off CHM model with an elongated prediction over the highway. The other prediction models do not

predict the rails holding road signs as a tree.

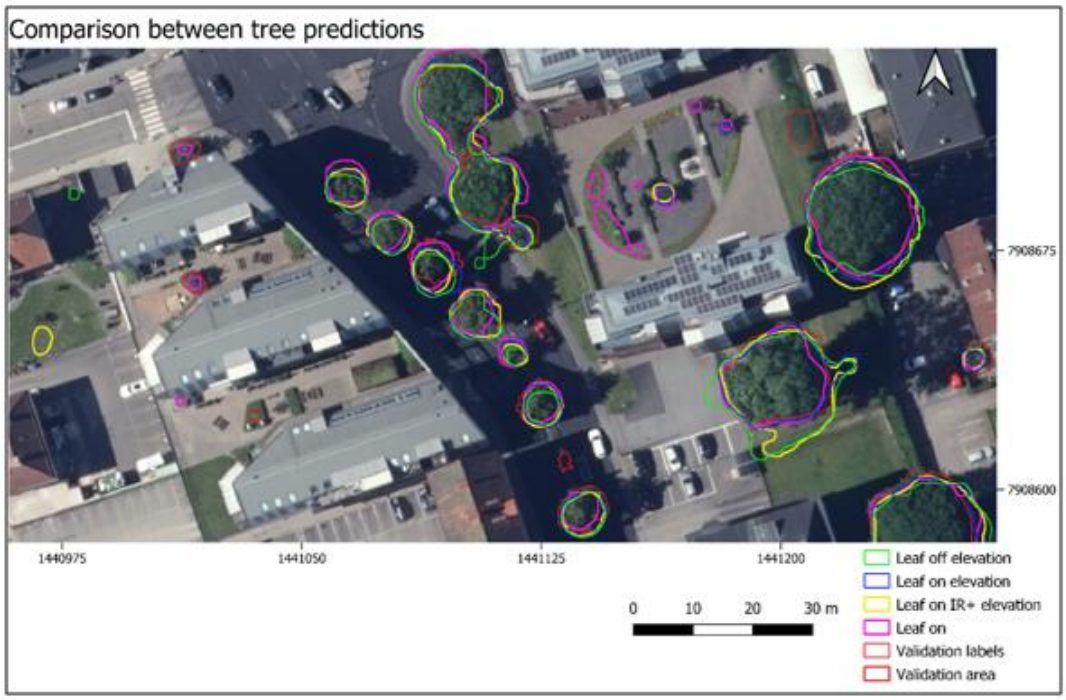

Figure 22. Various tree locations predicted by different model setups.

Figure 23 shows 10 epochs and the progress of the F1-score for every epoch for the 4 models with highest overall accuracy. The F1 score is increasing most for the R,G,B leaf-on model.

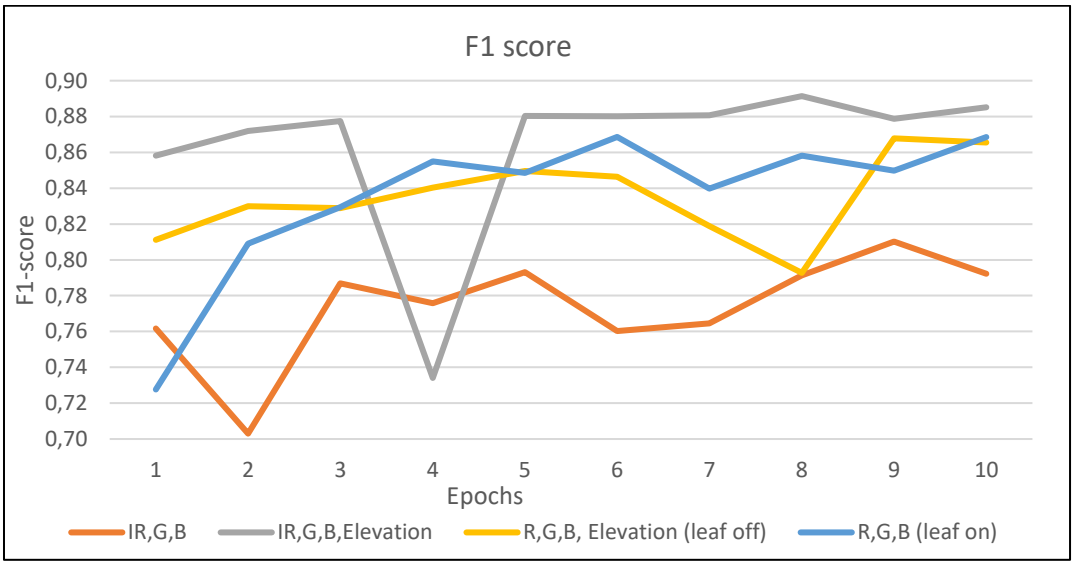

Figure 23. F1-score during 10 epochs for the band combinations with highest accuracy.

Figure 24 shows 10 epochs and the progress of the precision for every epoch for the 4 models with highest overall accuracy. The F1 score is increasing most for the IR,G,B leaf-on model.

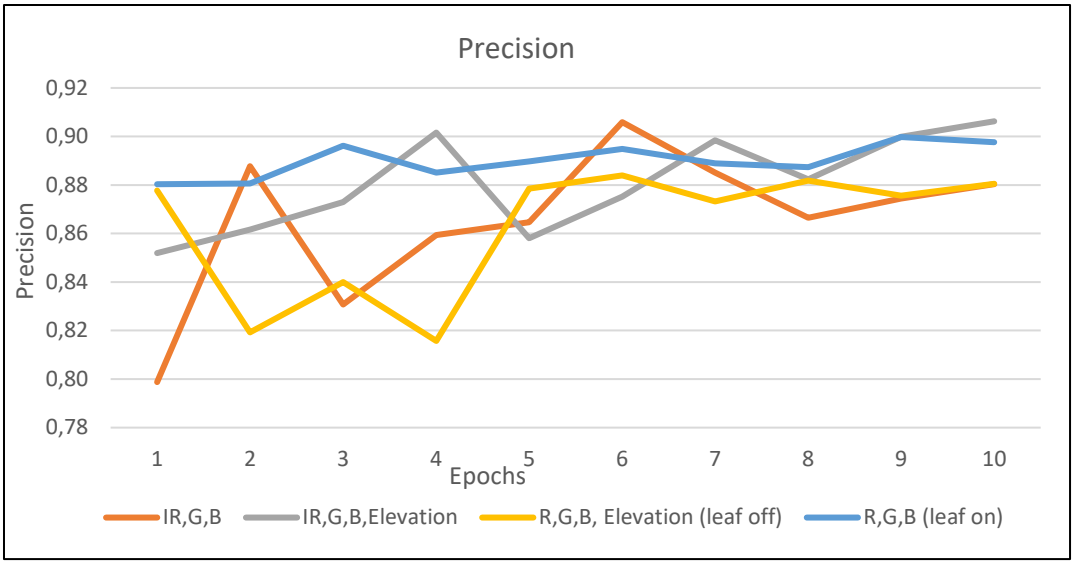

Figure 24. Precision during 10 epochs for the band combinations with highest accuracy.

4 Discussion

Lantmäteriet takes leaf-off imagery every 4th year and leaf-on imagery every 4th year (image acquisition every 2nd year). LIDAR scanning is preferable done leaf-off to detect other objects for city planning. Always perfect data is not realistic or can be financially defended, but can leaf-off images with LIDAR be used instead? The objective of this thesis was to evaluate the prediction accuracy and to identify the strengths and weaknesses in the deep learning model. The deep learning method using LIDAR and aerial leaf-off images had a F1-score of 87% and a precision of 88% mapping urban tree canopy. The combination of leaf-on data with IR and CHM scored the highest accuracy with a F1-score of 89% and a precision of 91%. The findings of this study indicates that tree canopy mapping with aerial images taken under leaf-off conditions is an applicable method in comparison with other methods. There was some prediction issues with rails holding road signs, but the model predicted trees in shadowy areas with the aid of the CHM. The results of this study indicate that LIDAR data seems to increase the prediction accuracy in shadowy areas.

4.1 Prediction issues

The prediction errors with rails holding road signs could be related to incorrect interpretation of LIDAR data. High objects not classified as buildings are more difficult to distinguish from vegetation (Lindberg et al., 2013) . Road sign rails crossing highways are such elements. This could affect the predictions, especially if a tree canopy is close to the rails. The method could possibly be developed with filters removing road sign rails from vegetation in the LIDAR data, by pre-processing LIDAR data with filters to refine the input in the model. Anyhow the leaf-on data in combination with LIDAR doesn´t predict road sign rails incorrect (Figure 22). Further studies could be made to validate this.

4.2 LIDAR and shadowy areas

Based on the results of this study, LIDAR seems to tackle the problems occurring when only RGB images are used, e.g. building shadow and colour related errors. Using only RGB images seems to yield less accurate results with problems such as other similar objects as bushes classified as trees (G. B. Martins et al., 2021). Other problems using only RGB-images may be the prediction errors related to the shape of the tree canopy edges, since they tend to have a less defined border without height information (G. B. Martins et al., 2021). Tree canopy cover was mapped in Central park, New York, using only RGB images (Yang et al., 2022). Darker shadows of tall buildings were an issue, resulting in undetected tree crowns. Such problems were found in this study, but less obvious with the CHM band added. The fusion of aerial and CHM data, combining the potential of both data sources, is a successful approach according to the results in this study. However, the LIDAR data should have at least 10 points per square meter to be useful for urban tree mapping (Katz et al., 2020). The use of LIDAR in this study seems to solve many of the issues with classification errors reported from other

similar studies. Tree canopy could be detected despite shadow from high buildings covering one side of the street. LIDAR data in combination with pléiades satellite images (Pu and Landry, 2020) was used with machine learning algorithms. The results showed that height information extracted from LIDAR data is helpful for improving the mapping of urban tree species. This study confirms that LIDAR height information is of value for urban tree detection, especially in shadowy areas. The watershed algorithm used in this study, based on LIDAR data, is probably an aid to create sharp edges of tree canopy as it adds important information to the classification.

Some remote sensing studies used a combination of LIDAR, aerial images and information from the near infrared (Banzhaf et al., 2018; Hanssen et al., 2021). However, using vegetation indices and IR information with leaf-off images could easily lead to an underestimation of tree canopy cover and was therefore only tested leaf-on in this study. Testing the use of different image resolutions is something that could be studied further. Higher image resolution might detect trees better, but the CHM with height values must be dense enough to use in combination with the aerial image.

Stadsträd, a Swedish remote sensing company, working with urban tree mapping, is using a similar method to collect training data as in this thesis. Their method is based on LIDAR-point clouds, e.g. with the open source data Laserdata skog (from Lantmäteriet) with a point density of 1–2 points/m2 and building polygons as input (S. Wiman, Stadsträd, personal communication, December 13, 2022).

Local maxima is calculated on the elevation data for all trees above 5 meters above ground. Trees are sorted in two classes, “possible building geometry” and “potential tree”. Manual control are done with aerial images in combination with object height data. This can be a time consuming task depending on both the nature of the input data and the variation of the trees in different areas.

The issues may be

- Early LIDAR acquisition date causing large trees, with or without several trunks as mistaken for several smaller trees. If the tree crowns are not dense enough to return LIDAR pulses, these trees may appear incorrect in the elevation model (varying heights).
- Exploitation of surfaces or clearings after the time of LIDAR acquisition date. Disappeared trees are visible in old elevation data.
- Too few trees in contiguous forest areas – tree crowns merge into each other and cannot be distinguished.

Stadsträd is doing an object detection of trees while this thesis is about conducting a semantic segmentation. The method of Stadsträd is human labour intensive and based on personal knowledge for tree delineation while the method stated in this thesis is automatic after training data has been collected. It is hard to compare the two methods since the method of Stadsträd of accuracy is relative the amount of human labour put in.

The benefits of object detection are that individual crown diameter and tree height can be obtained. But the accuracy in dense forest stands and the risk of over- or underestimation of individual trees are some problems related to object classification.

4.3 Limitations

Trees that have been cleared in between the acquisition of the LIDAR data and the aerial images may have been classified as trees. On the other hand, those planted after the acquisition of LIDAR data (2016) and taller than four metres during the acquisition of the aerial images might not been classified as trees. Tree crown area size could be underestimated both under leaf-off conditions and with LIDAR data from 2016, in particular with younger trees present in the aerial images. Underestimations of canopy area could lead to underestimations of calculations regarding $C0_2$ uptake and other metrics based on urban tree canopy cover.

The fact that LIDAR data is increasing the accuracy is a limitation. This could be a problem in smaller municipalities with a limited budget not allowing a LIDAR scanning. It could also be a problem if the LIDAR scanning is not up to date due to temporal differences with the aerial image, e.g. the data is mismatching. The possibility to use the suggested approach on another geographical site may be even higher only using only 3 channels as input; R,G,B. Point cloud data is however common data for most larger Swedish cities and seems to add higher value of accuracy to the model. If using RGB images only, the results of this study indicate that using images closer to the peak of the vegetation season would result in a higher accuracy.

4.4 Conclusions & Recommendations

The objectives to evaluate the deep learning model predictions has been detailed examined in this study by using a validation test, but also by looking at different types of trees, e.g. single trees, dense tree stands, small trees and large trees. Challenges, e.g. shadows and road sign rails have also been investigated.

The outcome of this thesis is that elevation data (CHM) is favourable to use with leaf-off data to increase tree mapping accuracy. The F1-score for leaf-off data increased from 68% to 88% when an extra band with CHM was added to the model. The elevation data is also favourable for IR and leaf-on data accuracy. This method is applicable to map urban tree canopy in a fast and accurate way, but possible improvements could be made using data LIDAR and aerial images with closer acquisition dates.

As an alternative of semantic segmentation used in this study, deep learning with object detection for trees is another field that could be further explore. This could add value in the work with green infrastructure as individual tree prediction is interesting for tree counts and urban tree plans on a detailed level. The challenges are difficulties with dense tree stands related to accuracy with object detection (Zhang et al., 2022).

The prediction models were tested in a dense urban area similar to the environment where the model was trained. Further studies and work must be made to train with more data and test the models in a larger area or a more heterogeneous urban structure regarding buildings and tree canopy.

The suggested approach of this thesis can add input value to the field of green infrastructure as it maps the current state of urban tree cover in a fast and accurate way. The method has the benefit of being open source and with a low threshold to get started without previous knowledge.

5 References

A Gentle Introduction to Pooling Layers for Convolutional Neural Networks - MachineLearningMastery.com [WWW Document], 2023. URL https://machinelearningmastery.com/pooling-layers-for-convolutional-neural-networks/ (accessed 2.1.23).

Abdi, A.M., 2020. Land cover and land use classification performance of machine learning algorithms in a boreal landscape using Sentinel-2 data. GIScience Remote Sens. 57, 1–20. https://doi.org/10.1080/15481603.2019.1650447/SUPPL_FILE/TGRS_A_1650447_SM9050.PDF

ASPRS - American Society for Photogrammetry & Remote Sensing, 2002. LAS Specification 1.4-R14 Release Information.

Astell-Burt, T., Feng, X., 2019. Association of Urban Green Space with Mental Health and General Health among Adults in Australia. JAMA Netw. Open. https://doi.org/10.1001/jamanetworkopen.2019.8209

Balikçi, S., Giezen, M., Arundel, R., 2022. The paradox of planning the compact and green city: analyzing land-use change in Amsterdam and Brussels. J. Environ. Plan. Manag. 65. https://doi.org/10.1080/09640568.2021.1971069

Banzhaf, E., Kollai, H., Kindler, A., 2018. Mapping urban grey and green structures for liveable cities using a 3D enhanced OBIA approach and vital statistics. https://doi.org/10.1080/10106049.2018.1524514 35, 623–640. https://doi.org/10.1080/10106049.2018.1524514

Blaschke, T., Hay, G.J., Kelly, M., Lang, S., Hofmann, P., Addink, E., Queiroz Feitosa, R., van der Meer, F., van der Werff, H., van Coillie, F., Tiede, D., 2014. Geographic Object-Based Image Analysis - Towards a new paradigm. ISPRS J. Photogramm. Remote Sens. https://doi.org/10.1016/j.isprsjprs.2013.09.014

Bosch, C.K. van den, 2021. Promoting health and wellbeing through urban forests – Introducing the 3-30-300 rule. Iucn.

Choi, R.Y., Coyner, A.S., Kalpathy-Cramer, J., Chiang, M.F., Peter Campbell, J., 2020. Introduction to Machine Learning, Neural Networks, and Deep Learning. Transl. Vis. Sci. Technol. 9, 14–14. https://doi.org/10.1167/TVST.9.2.14

Convolutional Neural Network Tutorial [Update] [WWW Document], 2023. URL https://www.simplilearn.com/tutorials/deep-learning-tutorial/convolutional-neural-network#GoTop (accessed 2.1.23).

Data Preparation in Machine Learning: 6 Key Steps [WWW Document], 2023. URL https://www.techtarget.com/searchbusinessanalytics/feature/Data-preparation-in-machine-learning-6-key-steps (accessed 1.27.23).

de la Barrera, F., Reyes-Paecke, S., Truffello, R., de la Fuente, H., Salinas, V., Villegas, R., Steiniger, S., 2023. Comparing green spaces provision and accessibility indicators over a latitudinal gradient and multiple climate zones. Urban For. Urban Green. 79, 127791. https://doi.org/10.1016/J.UFUG.2022.127791

Deneke, F., 1993. Proceedings of the First Canadian Urban Forests Conference May 30- June 2, 1993, in: Urban Forestry in North America: Towards a Global Ecosystem Perspective. Blouin & R. Comeau, p. 151.

Descending into ML: Training and Loss | Machine Learning Crash Course | Google Developers [WWW Document], 2022. URL https://developers.google.com/machine-learning/crash-course/descending-into-ml/training-and-loss (accessed 7.10.22).
Fick, S.E., Hijmans, R.J., 2017. WorldClim 2: new 1-km spatial resolution climate surfaces for global land areas. Int. J. Climatol. https://doi.org/10.1002/joc.5086
Fletcher, D.H., Garrett, J.K., Thomas, A., Fitch, A., Cryle, P., Shilton, S., Jones, L., 2022. Location, Location, Location: Modelling of Noise Mitigation by Urban Woodland Shows the Benefit of Targeted Tree Planting in Cities. Sustainability 14, 7079. https://doi.org/10.3390/su14127079
Hanssen, F., Barton, D.N., Venter, Z.S., Nowell, M.S., Cimburova, Z., 2021. Utilizing LiDAR data to map tree canopy for urban ecosystem extent and condition accounts in Oslo. Ecol. Indic. 130, 108007. https://doi.org/10.1016/J.ECOLIND.2021.108007
Hartling, S., Sagan, V., Sidike, P., Maimaitijiang, M., Carron, J., 2019. Urban Tree Species Classification Using a WorldView-2/3 and LiDAR Data Fusion Approach and Deep Learning. https://doi.org/10.3390/s19061284
Hayes, A.T., Jandaghian, Z., Lacasse, M.A., Gaur, A., Lu, H., Laouadi, A., Ge, H., Wang, L., 2022. Nature-Based Solutions (NBSs) to Mitigate Urban Heat Island (UHI) Effects in Canadian Cities. Buildings 12, 925. https://doi.org/10.3390/buildings12070925
He, K., Zhang, X., Ren, S., Sun, J., 2016. Deep residual learning for image recognition, in: Proceedings of the IEEE Computer Society Conference on Computer Vision and Pattern Recognition. https://doi.org/10.1109/CVPR.2016.90
Heller, RC., 1964. Identification of Tree Species on Large-scale Panchromatic and Color Aerial Photographs. US Department of Agriculture, Forest Service.
i-Tree Eco Field Guide 4.26.2016, 2016.
Karimi, A., Nasiri, S., Kazerooni, F., Oliaei, M., 2010. Noise induced hearing loss risk assessment in truck drivers. Noise Health 12, 49. https://doi.org/10.4103/1463-1741.59999
Katz, D.S.W., Batterman, S.A., Brines, S.J., 2020. Improved Classification of Urban Trees Using a Widespread Multi-Temporal Aerial Image Dataset. Remote Sens. 12, 2475. https://doi.org/10.3390/rs12152475
Khosravipour, A., Skidmore, A.K., Isenburg, M., Wang, T., Hussin, Y.A., 2014. Generating pit-free canopy height models from airborne lidar. Photogramm. Eng. Remote Sens. https://doi.org/10.14358/PERS.80.9.863
Khreis, H., Warsow, K.M., Verlinghieri, E., Guzman, A., Pellecuer, L., Ferreira, A., Jones, I., Heinen, E., Rojas-Rueda, D., Mueller, N., Schepers, P., Lucas, K., Nieuwenhuijsen, M., 2016. The health impacts of traffic-related exposures in urban areas: Understanding real effects, underlying driving forces and co-producing future directions. J. Transp. Health 3, 249–267. https://doi.org/10.1016/J.JTH.2016.07.002
Lantmäteriet, 2017. Flygfotografering, HMK – handbok i mät- och kartfrågor.
Lin, J., Kroll, C.N., Nowak, D.J., Greenfield, E.J., 2019. A review of urban forest modeling: Implications for management and future research. Urban For. Urban Green. 43, 126366. https://doi.org/10.1016/J.UFUG.2019.126366
Lindberg, F., Johansson, L., Thorsson, S., 2013. LiDAR-data för att identifiera urban vegetation.
Ma, L., Liu, Y., Zhang, X., Ye, Y., Yin, G., Johnson, B.A., 2019. Deep learning in remote sensing applications: A meta-analysis and review. ISPRS J. Photogramm. Remote Sens. 152, 166–177. https://doi.org/10.1016/J.ISPRSJPRS.2019.04.015

Martins, G.B., La Rosa, L.E.C., Happ, P.N., Filho, L.C.T.C., Santos, C.J.F., Feitosa, R.Q., Ferreira, M.P., 2021. Deep learning-based tree species mapping in a highly diverse tropical urban setting. Urban For. Urban Green. 64, 127241. https://doi.org/10.1016/J.UFUG.2021.127241

Martins, J.A.C., Nogueira, K., Osco, L.P., Gomes, F.D.G., Furuya, D.E.G., Gonçalves, W.N., Sant'Ana, D.A., Ramos, A.P.M., Liesenberg, V., dos Santos, J.A., de Oliveira, P.T.S., Junior, J.M., 2021. Semantic Segmentation of Tree-Canopy in Urban Environment with Pixel-Wise Deep Learning. Remote Sens. 13, 3054. https://doi.org/10.3390/rs13163054

Myint, S.W., Gober, P., Brazel, A., Grossman-Clarke, S., Weng, Q., 2011. Per-pixel vs. object-based classification of urban land cover extraction using high spatial resolution imagery. Remote Sens. Environ. 115, 1145–1161. https://doi.org/10.1016/J.RSE.2010.12.017

Oke, T.R., 1982. The energetic basis of the urban heat island. Q. J. R. Meteorol. Soc. 108, 1–24. https://doi.org/10.1002/QJ.49710845502

Ondruska, P., Dequaire, J., Wang, D., arXiv, I.P.- arXiv preprint, 2016, undefined, 2016. End-to-end tracking and semantic segmentation using recurrent neural networks. arxiv.org.

Probabilistic losses [WWW Document], 2023. URL https://keras.io/api/losses/probabilistic_losses/#binarycrossentropy-class. (accessed 2.2.23).

Prudencio, L., Null, S.E., 2018. Stormwater management and ecosystem services: a review. Environ. Res. Lett. 13, 033002. https://doi.org/10.1088/1748-9326/AAA81A

Pu, R., Landry, S., 2020. Mapping urban tree species by integrating multi-seasonal high resolution pléiades satellite imagery with airborne LiDAR data. Urban For. Urban Green. 53, 126675. https://doi.org/10.1016/J.UFUG.2020.126675

Pyo, S., Lee, J., Cha, M., Jang, H., 2017. Predictability of machine learning techniques to forecast the trends of market index prices: Hypothesis testing for the Korean stock markets. PLoS ONE 12. https://doi.org/10.1371/JOURNAL.PONE.0188107

Qian, R., Zhang, B., Yue, Y., … Z.W.-2015 11th I., 2015, undefined, 2015. Robust Chinese traffic sign detection and recognition with deep convolutional neural network. ieeexplore.ieee.org 2016-January, 791–796. https://doi.org/10.1109/ICNC.2015.7378092

Ressl, C., Mandlburger, G., Pfeifer, N., 2009. Investigating adjustment of airborne laser scanning strips without usage of GNSS/IMU trajectory data. Laser Scanning 2009 38.

Richards, J.A., Jia, X., 1999. Remote Sensing Digital Image Analysis, Remote Sensing Digital Image Analysis. https://doi.org/10.1007/978-3-662-03978-6

Rouse, J.W., Haas, R.H., Schell, J.A., Deering, D.W., 1973. Monitoring the vernal advancement and retrogradation (green wave effect) of natural vegetation. Prog. Rep. RSC 1978-1.

Tao, D., Zhang, D., Hu, R., Rundensteiner, E., Feng, H., 2021. Crowdsourcing and machine learning approaches for extracting entities indicating potential foodborne outbreaks from social media. Sci. Rep. 2021 111 11, 1–12. https://doi.org/10.1038/s41598-021-00766-w

Timilsina, S., Aryal, J., Kirkpatrick, J.B., 2020. Mapping urban tree cover changes using object-based convolution neural network (OB-CNN). Remote Sens. 12. https://doi.org/10.3390/RS12183017

Van Renterghem, T., 2014. Guidelines for optimizing road traffic noise shielding by non-deep tree belts. Ecol. Eng. 69, 276–286. https://doi.org/10.1016/J.ECOLENG.2014.04.029

Vauhkonen, J., Ørka, H.O., Holmgren, J., Dalponte, M., Heinzel, J., Koch, B., 2014. Tree Species Recognition Based on Airborne Laser Scanning and Complementary Data Sources 135–156. https://doi.org/10.1007/978-94-017-8663-8_7

Wang, Z., Fan, C., Xian, M., 2021. Application and evaluation of a deep learning architecture to urban tree canopy mapping. Remote Sens. 13, 1–14. https://doi.org/10.3390/rs13091749

What are containers? | Google Cloud [WWW Document], 20230131. URL https://cloud.google.com/learn/what-are-containers (accessed 2.1.23).

What is Deep Learning? | IBM [WWW Document], 2020. URL https://www.ibm.com/cloud/learn/deep-learning (accessed 5.5.22).

With, K.A., With, K.A., 2019. Landscape Connectivity, in: Essentials of Landscape Ecology. https://doi.org/10.1093/oso/9780198838388.003.0005

Witten, I., Frank, E., 2023. Data Mining: Practical Machine Learning Tools and Techniques, Second Edition - [WWW Document]. URL https://books.google.se/books?id=QTnOcZJzlUoC&pg=PA172&lpg=PA172&dq=precision+tp&source=bl&ots=3jnBasYjNf&sig=ACfU3U1pTR3Cuw3STXweaSrMh142WJBA7w&hl=en&sa=X&ved=2ahUKEwjkq5KRqPX8AhX3i_0HHRSLBR0Q6AF6BAguEAM#v=onepage&q=precision%20tp&f=false (accessed 2.1.23).

Yang, M., Mou, Y., Liu, S., Meng, Y., Liu, Z., Li, P., Xiang, W., Zhou, X., Peng, C., 2022. Detecting and mapping tree crowns based on convolutional neural network and Google Earth images. Int. J. Appl. Earth Obs. Geoinformation 108, 102764. https://doi.org/10.1016/J.JAG.2022.102764

Zhang, L., Lin, H., Wang, F., 2022. Individual Tree Detection Based on High-Resolution RGB Images for Urban Forestry Applications. https://doi.org/10.1109/ACCESS.2022.3171585

6 Appendix

R-code

Creation of CHM

```
.libPaths( c( "C:/Users/Public/R/win-library/4.2" , .libPaths() ) )
library(lidR)
# Path to data
LASfile <- ("path/file.las")
# Sorting out points in point cloud data, keeping vegetation and ground point classes.
las <- readLAS(LASfile, filter="-keep_class 1 2") # Keep high vegetation and ground point classes

# Normalizing ground points to 0 elevation (idwinterpolation), instead of meters above sea level.
dtm <- grid_terrain(las, algorithm = knnidw(k = 8, p = 2))
las_normalized <- normalize_height(las, dtm)
# Create a filter to remove points above 95th percentile of height
lasfilternoise = function(las, sensitivity)
{
  p95 <- grid_metrics(las, ~quantile(Z, probs = 0.95), 10)
  las <- merge_spatial(las, p95, "p95")
  las <- filter_poi(las, Z < p95*sensitivity)
  las$p95 <- NULL
  return(las)
}
# Generating a pitfree canopy height model without null values (Khosravipour et al., 2014)
las_denoised <- lasfilternoise(las_normalized, sensitivity = 1.2)
chm <- grid_canopy(las_denoised, 0.32, pitfree(c(0,2,5,10,15), c(3,1.5), subcircle = 0.2))
# Applying a median filter, 3x3 moving window to smooth the image and remove noise
ker <- matrix(1,3,3)
chms <- raster::focal(chm, w = ker, fun = median)
library(raster)
# Writing output file
writeRaster(chms, filename="path/file.asc", format="ascii", overwrite=TRUE)
citation("lidR")
#> Roussel, J.R., Auty, D., Coops, N. C., Tompalski, P., Goodbody, T. R. H., Sánchez Meador, A., Bourdon, J.F., De Boissieu, F., Achim, A. (2020). lidR : An R package for analysis of Airborne Laser Scanning (ALS) data. Remote Sensing of Environment, 251 (August), 112061. <doi:10.1016/j.rse.2020.112061>.
#> Jean-Romain Roussel and David Auty (2021). Airborne LiDAR Data Manipulation and Visualization for Forestry Applications. R package version 3.1.0. https://cran.r-project.org/package=lidR
```

Hull generation

```
.libPaths( c( "C:/Users/Public/R/win-library/4.2" , .libPaths() ) )
library(lidR)
# Path to data
LASfile <- ("path/file.las")
# Sorting out points in point cloud data, keeping vegetation and ground point classes.
las <- readLAS(LASfile, filter="-keep_class 1 2") # Keep high vegetation and ground point classes

# Normalizing ground points to 0 elevation (idwinterpolation), instead of meters above sea level.
dtm <- grid_terrain(las, algorithm = knnidw(k = 8, p = 2))
las_normalized <- normalize_height(las, dtm)
# Create a filter to remove points above 95th percentile of height
lasfilternoise = function(las, sensitivity)
{
  p95 <- grid_metrics(las, ~quantile(Z, probs = 0.95), 10)
  las <- merge_spatial(las, p95, "p95")
  las <- filter_poi(las, Z < p95*sensitivity)
  las$p95 <- NULL
  return(las)
}
# Generating a pitfree canopy height model without null values (Khosravipour et al., 2014)
las_denoised <- lasfilternoise(las_normalized, sensitivity = 1.2)
chm <- grid_canopy(las_denoised, 0.32, pitfree(c(0,2,5,10,15), c(3,1.5), subcircle = 0.2))
# Applying a median filter, 3x3 moving window to smooth the image and remove noise
ker <- matrix(1,3,3)
chm_s <- raster::focal(chm,th = 4, w = ker, fun = mean, na.rm = TRUE)
las_watershed <- segment_trees(las, watershed(chm_s))
# Removing points that are not assigned to a tree
trees <- filter_poi(las_watershed, !is.na(treeID))
hulls <- delineate_crowns(trees, type = "concave", concavity = 2, func =
.stdmetrics)
plot(hulls)
plot(chm_s)
require(rgdal)
require(rgeos)
writeOGR(hulls,"path/","filename", driver = "ESRI Shapefile")
```

Python code, raster vision

```
import os
from os.path import join, basename

from rastervision.core.rv_pipeline import *
from rastervision.core.backend import *
from rastervision.core.data import *
from rastervision.core.analyzer import *
from rastervision.pytorch_backend import *
from rastervision.pytorch_learner import *
from rastervision.pytorch_backend.examples.utils import (get_scene_info,
                                        save_image_crop)
from rastervision.pytorch_backend.examples.semantic_segmentation.utils import (
    example_multiband_transform, example_rgb_transform, imagenet_stats,
    Unnormalize)



def get_config(runner,
               multiband: bool = True,
               external_model: bool = False,
               augment: bool = False,
               nochip: bool = False,
               test: bool = False):
    root_uri = '/opt/data/output/'
    train_image_uris = ['/opt/data/data_input/images/1.tif']
    train_label_uris = ['/opt/data/data_input/labels/1.geojson']
    train_scene_ids = ['1']
    train_scene_list = list(zip(train_scene_ids, train_image_uris, train_label_uris))

    val_image_uri = '/opt/data/data_input/images/2.tif'
    val_label_uri = '/opt/data/data_input/labels/2.geojson'
    val_scene_id = '2'
```

```
train_scenes_input = []

channel_order = [0, 1, 2,3]
channel_display_groups = None
aug_transform = example_rgb_transform

if augment:
    mu, std = imagenet_stats['mean'], imagenet_stats['std']
    mu, std = mu[channel_order], std[channel_order]

    base_transform = A.Normalize(mean=mu.tolist(), std=std.tolist())
    plot_transform = Unnormalize(mean=mu, std=std)

    aug_transform = A.to_dict(aug_transform)
    base_transform = A.to_dict(base_transform)
    plot_transform = A.to_dict(plot_transform)
else:
    aug_transform = None
    base_transform = None
    plot_transform = None

chip_sz = 300
img_sz = chip_sz
if nochip:
    chip_options = SemanticSegmentationChipOptions()
else:
    chip_options = SemanticSegmentationChipOptions(
        window_method=SemanticSegmentationWindowMethod.sliding,
        stride=chip_sz)

class_config = ClassConfig(
names=['tree', 'background'], colors=['red', 'black'])

def make_scene(scene_id, image_uri, label_uri):
```

```
    raster_source = RasterioSourceConfig(
        uris=[image_uri],
        channel_order=channel_order,
        transformers=[StatsTransformerConfig()])
    vector_source = GeoJSONVectorSourceConfig(
        uri=label_uri, transformers=[ClassInferenceTransformerConfig(default_class_id=0)],
ignore_crs_field=True)
    label_source = SemanticSegmentationLabelSourceConfig(
        raster_source=RasterizedSourceConfig(
            vector_source=vector_source,
            rasterizer_config=RasterizerConfig(background_class_id=1)))

    label_store = SemanticSegmentationLabelStoreConfig(
        rgb=True, vector_output=[PolygonVectorOutputConfig(class_id=0)])
    return SceneConfig(
        id=scene_id,
        raster_source=raster_source,
        label_source=label_source,
        label_store=label_store)



for scene in train_scene_list:
    train_scenes_input.append(make_scene(*scene))

dataset = DatasetConfig(
class_config=class_config,
train_scenes=
    train_scenes_input
,
validation_scenes=[
    make_scene(val_scene_id, val_image_uri, val_label_uri)
])

chip_sz = 300
```

```
    backend = PyTorchSemanticSegmentationConfig(
        data=SemanticSegmentationImageDataConfig(img_channels=len(channel_order), img_sz=img_sz),
        model=SemanticSegmentationModelConfig(backbone=Backbone.resnet50),
        solver=SolverConfig(lr=1e-4, num_epochs=10, batch_sz=4))
    chip_options =
SemanticSegmentationChipOptions(window_method=SemanticSegmentationWindowMethod.sliding)


    return SemanticSegmentationConfig(
        root_uri=root_uri,
        dataset=dataset,
        backend=backend,
        train_chip_sz=chip_sz,
        predict_chip_sz=chip_sz)
```

Series from Lund University

Department of Physical Geography and Ecosystem Science

Master Thesis in Geographical Information Science

1. *Anthony Lawther:* The application of GIS-based binary logistic regression for slope failure susceptibility mapping in the Western Grampian Mountains, Scotland (2008).
2. *Rickard Hansen:* Daily mobility in Grenoble Metropolitan Region, France. Applied GIS methods in time geographical research (2008).
3. *Emil Bayramov:* Environmental monitoring of bio-restoration activities using GIS and Remote Sensing (2009).
4. *Rafael Villarreal Pacheco:* Applications of Geographic Information Systems as an analytical and visualization tool for mass real estate valuation: a case study of Fontibon District, Bogota, Columbia (2009).
5. *Siri Oestreich Waage:* a case study of route solving for oversized transport: The use of GIS functionalities in transport of transformers, as part of maintaining a reliable power infrastructure (2010).
6. *Edgar Pimiento:* Shallow landslide susceptibility – Modelling and validation (2010).
7. *Martina Schäfer:* Near real-time mapping of floodwater mosquito breeding sites using aerial photographs (2010).
8. *August Pieter van Waarden-Nagel:* Land use evaluation to assess the outcome of the programme of rehabilitation measures for the river Rhine in the Netherlands (2010).
9. *Samira Muhammad:* Development and implementation of air quality data mart for Ontario, Canada: A case study of air quality in Ontario using OLAP tool. (2010).
10. *Fredros Oketch Okumu*: Using remotely sensed data to explore spatial and temporal relationships between photosynthetic productivity of vegetation and malaria transmission intensities in selected parts of Africa (2011).
11. *Svajunas Plunge:* Advanced decision support methods for solving diffuse water pollution problems (2011).
12. *Jonathan Higgins:* Monitoring urban growth in greater Lagos: A case study using GIS to monitor the urban growth of Lagos 1990 - 2008 and produce future growth prospects for the city (2011).
13. *Mårten Karlberg:* Mobile Map Client API: Design and Implementation for Android (2011).

14. *Jeanette McBride:* Mapping Chicago area urban tree canopy using color infrared imagery (2011).

15. *Andrew Farina:* Exploring the relationship between land surface temperature and vegetation abundance for urban heat island mitigation in Seville, Spain (2011).

16. *David Kanyari*: Nairobi City Journey Planner: An online and a Mobile Application (2011).

17. *Laura V. Drews:* Multi-criteria GIS analysis for siting of small wind power plants - A case study from Berlin (2012).

18. *Qaisar Nadeem:* Best living neighborhood in the city - A GIS based multi criteria evaluation of ArRiyadh City (2012).

19. *Ahmed Mohamed El Saeid Mustafa:* Development of a photo voltaic building rooftop integration analysis tool for GIS for Dokki District, Cairo, Egypt (2012).

20. *Daniel Patrick Taylor*: Eastern Oyster Aquaculture: Estuarine Remediation via Site Suitability and Spatially Explicit Carrying Capacity Modeling in Virginia's Chesapeake Bay (2013).

21. *Angeleta Oveta Wilson:* A Participatory GIS approach to *unearthing* Manchester's Cultural Heritage '*gold mine'* (2013).

22. *Ola Svensson:* Visibility and Tholos Tombs in the Messenian Landscape: A Comparative Case Study of the Pylian Hinterlands and the Soulima Valley (2013).

23. *Monika Ogden:* Land use impact on water quality in two river systems in South Africa (2013).

24. *Stefan Rova:* A GIS based approach assessing phosphorus load impact on Lake Flaten in Salem, Sweden (2013).

25. *Yann Buhot:* Analysis of the history of landscape changes over a period of 200 years. How can we predict past landscape pattern scenario and the impact on habitat diversity? (2013).

26. *Christina Fotiou:* Evaluating habitat suitability and spectral heterogeneity models to predict weed species presence (2014).

27. *Inese Linuza:* Accuracy Assessment in Glacier Change Analysis (2014).

28. *Agnieszka Griffin:* Domestic energy consumption and social living standards: a GIS analysis within the Greater London Authority area (2014).

29. *Brynja Guðmundsdóttir:* Detection of potential arable land with remote sensing and GIS - A Case Study for Kjósarhreppur (2014).

30. *Oleksandr Nekrasov:* Processing of MODIS Vegetation Indices for analysis of agricultural droughts in the southern Ukraine between the years 2000-2012 (2014).

31. *Sarah Tressel:* Recommendations for a polar Earth science portal in the context of Arctic Spatial Data Infrastructure (2014).

32. *Caroline Gevaert:* Combining Hyperspectral UAV and Multispectral Formosat-2 Imagery for Precision Agriculture Applications (2014).

33. *Salem Jamal-Uddeen:* Using GeoTools to implement the multi-criteria evaluation analysis - weighted linear combination model (2014).

34. *Samanah Seyedi-Shandiz:* Schematic representation of geographical railway network at the Swedish Transport Administration (2014).

35. *Kazi Masel Ullah:* Urban Land-use planning using Geographical Information System and analytical hierarchy process: case study Dhaka City (2014).

36. *Alexia Chang-Wailing Spitteler:* Development of a web application based on MCDA and GIS for the decision support of river and floodplain rehabilitation projects (2014).

37. *Alessandro De Martino:* Geographic accessibility analysis and evaluation of potential changes to the public transportation system in the City of Milan (2014).

38. *Alireza Mollasalehi:* GIS Based Modelling for Fuel Reduction Using Controlled Burn in Australia. Case Study: Logan City, QLD (2015).

39. *Negin A. Sanati:* Chronic Kidney Disease Mortality in Costa Rica; Geographical Distribution, Spatial Analysis and Non-traditional Risk Factors (2015).

40. *Karen McIntyre:* Benthic mapping of the Bluefields Bay fish sanctuary, Jamaica (2015).

41. *Kees van Duijvendijk:* Feasibility of a low-cost weather sensor network for agricultural purposes: A preliminary assessment (2015).

42. *Sebastian Andersson Hylander:* Evaluation of cultural ecosystem services using GIS (2015).

43. *Deborah Bowyer:* Measuring Urban Growth, Urban Form and Accessibility as Indicators of Urban Sprawl in Hamilton, New Zealand (2015).

44. *Stefan Arvidsson:* Relationship between tree species composition and phenology extracted from satellite data in Swedish forests (2015).

45. *Damián Giménez Cruz*: GIS-based optimal localisation of beekeeping in rural Kenya (2016).

46. *Alejandra Narváez Vallejo:* Can the introduction of the topographic indices in LPJ-GUESS improve the spatial representation of environmental variables? (2016).

47. *Anna Lundgren:* Development of a method for mapping the highest coastline in Sweden using breaklines extracted from high resolution digital elevation models (2016).

48. *Oluwatomi Esther Adejoro:* Does location also matter? A spatial analysis of social achievements of young South Australians (2016).

49. *Hristo Dobrev Tomov:* Automated temporal NDVI analysis over the Middle East for the period 1982 - 2010 (2016).

50. *Vincent Muller:* Impact of Security Context on Mobile Clinic Activities A GIS Multi Criteria Evaluation based on an MSF Humanitarian Mission in Cameroon (2016).

51. *Gezahagn Negash Seboka:* Spatial Assessment of NDVI as an Indicator of Desertification in Ethiopia using Remote Sensing and GIS (2016).

52. *Holly Buhler:* Evaluation of Interfacility Medical Transport Journey Times in Southeastern British Columbia. (2016).

53. *Lars Ole Grottenberg*: Assessing the ability to share spatial data between emergency management organisations in the High North (2016).

54. *Sean Grant:* The Right Tree in the Right Place: Using GIS to Maximize the Net Benefits from Urban Forests (2016).

55. *Irshad Jamal:* Multi-Criteria GIS Analysis for School Site Selection in Gorno-Badakhshan Autonomous Oblast, Tajikistan (2016).

56. *Fulgencio Sanmartín:* Wisdom-volkano: A novel tool based on open GIS and time-series visualization to analyse and share volcanic data (2016).

57. *Nezha Acil:* Remote sensing-based monitoring of snow cover dynamics and its influence on vegetation growth in the Middle Atlas Mountains (2016).

58. *Julia Hjalmarsson:* A Weighty Issue: Estimation of Fire Size with Geographically Weighted Logistic Regression (2016).

59. *Mathewos Tamiru Amato:* Using multi-criteria evaluation and GIS for chronic food and nutrition insecurity indicators analysis in Ethiopia (2016).

60. *Karim Alaa El Din Mohamed Soliman El Attar:* Bicycling Suitability in Downtown, Cairo, Egypt (2016).

61. *Gilbert Akol Echelai:* Asset Management: Integrating GIS as a Decision Support Tool in Meter Management in National Water and Sewerage Corporation (2016).

62. *Terje Slinning:* Analytic comparison of multibeam echo soundings (2016).

63. *Gréta Hlín Sveinsdóttir:* GIS-based MCDA for decision support: A framework for wind farm siting in Iceland (2017).

64. *Jonas Sjögren:* Consequences of a flood in Kristianstad, Sweden: A GIS-based analysis of impacts on important societal functions (2017).

65. *Nadine Raska:* 3D geologic subsurface modelling within the Mackenzie Plain, Northwest Territories, Canada (2017).

66. *Panagiotis Symeonidis*: Study of spatial and temporal variation of atmospheric optical parameters and their relation with PM 2.5 concentration over Europe using GIS technologies (2017).

67. *Michaela Bobeck:* A GIS-based Multi-Criteria Decision Analysis of Wind Farm Site Suitability in New South Wales, Australia, from a Sustainable Development Perspective (2017).

68. *Raghdaa Eissa*: Developing a GIS Model for the Assessment of Outdoor Recreational Facilities in New Cities Case Study: Tenth of Ramadan City, Egypt (2017).

69. *Zahra Khais Shahid*: Biofuel plantations and isoprene emissions in Svea and Götaland (2017).

70. *Mirza Amir Liaquat Baig*: Using geographical information systems in epidemiology: Mapping and analyzing occurrence of diarrhea in urban - residential area of Islamabad, Pakistan (2017).

71. *Joakim Jörwall*: Quantitative model of Present and Future well-being in the EU-28: A spatial Multi-Criteria Evaluation of socioeconomic and climatic comfort factors (2017).

72. *Elin Haettner*: Energy Poverty in the Dublin Region: Modelling Geographies of Risk (2017).

73. *Harry Eriksson*: Geochemistry of stream plants and its statistical relations to soil- and bedrock geology, slope directions and till geochemistry. A GIS-analysis of small catchments in northern Sweden (2017).

74. *Daniel Gardevärn:* PPGIS and Public meetings – An evaluation of public participation methods for urban planning (2017).

75. *Kim Friberg:* Sensitivity Analysis and Calibration of Multi Energy Balance Land Surface Model Parameters (2017).

76. *Viktor Svanerud:* Taking the bus to the park? A study of accessibility to green areas in Gothenburg through different modes of transport (2017).

77. *Lisa-Gaye Greene*: Deadly Designs: The Impact of Road Design on Road Crash Patterns along Jamaica's North Coast Highway (2017).

78. *Katarina Jemec Parker*: Spatial and temporal analysis of fecal indicator bacteria concentrations in beach water in San Diego, California (2017).

79. *Angela Kabiru*: An Exploratory Study of Middle Stone Age and Later Stone Age Site Locations in Kenya's Central Rift Valley Using Landscape Analysis: A GIS Approach (2017).

80. *Kristean Björkmann*: Subjective Well-Being and Environment: A GIS-Based Analysis (2018).

81. *Williams Erhunmonmen Ojo*: Measuring spatial accessibility to healthcare for people living with HIV-AIDS in southern Nigeria (2018).

82. *Daniel Assefa*: Developing Data Extraction and Dynamic Data Visualization (Styling) Modules for Web GIS Risk Assessment System (WGRAS). (2018).

83. *Adela Nistora*: Inundation scenarios in a changing climate: assessing potential impacts of sea-level rise on the coast of South-East England (2018).

84. *Marc Seliger*: Thirsty landscapes - Investigating growing irrigation water consumption and potential conservation measures within Utah's largest master-planned community: Daybreak (2018).

85. *Luka Jovičić*: Spatial Data Harmonisation in Regional Context in Accordance with INSPIRE Implementing Rules (2018).

86. *Christina Kourdounouli*: Analysis of Urban Ecosystem Condition Indicators for the Large Urban Zones and City Cores in EU (2018).

87. *Jeremy Azzopardi*: Effect of distance measures and feature representations on distance-based accessibility measures (2018).

88. *Patrick Kabatha*: An open source web GIS tool for analysis and visualization of elephant GPS telemetry data, alongside environmental and anthropogenic variables (2018).

89. *Richard Alphonce Giliba*: Effects of Climate Change on Potential Geographical Distribution of Prunus africana (African cherry) in the Eastern Arc Mountain Forests of Tanzania (2018).

90. *Eiður Kristinn Eiðsson*: Transformation and linking of authoritative multi-scale geodata for the Semantic Web: A case study of Swedish national building data sets (2018).

91. *Niamh Harty*: HOP!: a PGIS and citizen science approach to monitoring the condition of upland paths (2018).

92. *José Estuardo Jara Alvear*: Solar photovoltaic potential to complement hydropower in Ecuador: A GIS-based framework of analysis (2018).

93. *Brendan O'Neill*: Multicriteria Site Suitability for Algal Biofuel Production Facilities (2018).

94. *Roman Spataru*: Spatial-temporal GIS analysis in public health – a case study of polio disease (2018).

95. *Alicja Miodońska*: Assessing evolution of ice caps in Suðurland, Iceland, in years 1986 - 2014, using multispectral satellite imagery (2019).

96. *Dennis Lindell Schettini*: A Spatial Analysis of Homicide Crime's Distribution and Association with Deprivation in Stockholm Between 2010-2017 (2019).

97. *Damiano Vesentini*: The Po Delta Biosphere Reserve: Management challenges and priorities deriving from anthropogenic pressure and sea level rise (2019).

98. *Emilie Arnesten*: Impacts of future sea level rise and high water on roads, railways and environmental objects: a GIS analysis of the potential effects of increasing sea levels and highest projected high water in Scania, Sweden (2019).

99. *Syed Muhammad Amir Raza*: Comparison of geospatial support in RDF stores: Evaluation for ICOS Carbon Portal metadata (2019).

100. *Hemin Tofiq*: Investigating the accuracy of Digital Elevation Models from UAV images in areas with low contrast: A sandy beach as a case study (2019).

101. *Evangelos Vafeiadis*: Exploring the distribution of accessibility by public transport using spatial analysis. A case study for retail concentrations and public hospitals in Athens (2019).

102. *Milan Sekulic*: Multi-Criteria GIS modelling for optimal alignment of roadway by-passes in the Tlokweng Planning Area, Botswana (2019).

103. *Ingrid Piirisaar*: A multi-criteria GIS analysis for siting of utility-scale photovoltaic solar plants in county Kilkenny, Ireland (2019).

104. *Nigel Fox*: Plant phenology and climate change: possible effect on the onset of various wild plant species' first flowering day in the UK (2019).

105. *Gunnar Hesch*: Linking conflict events and cropland development in Afghanistan, 2001 to 2011, using MODIS land cover data and Uppsala Conflict Data Programme (2019).

106. *Elijah Njoku*: Analysis of spatial-temporal pattern of Land Surface Temperature (LST) due to NDVI and elevation in Ilorin, Nigeria (2019).

107. *Katalin Bunyevácz*: Development of a GIS methodology to evaluate informal urban green areas for inclusion in a community governance program (2019).

108. *Paul dos Santos*: Automating synthetic trip data generation for an agent-based simulation of urban mobility (2019).

109. *Robert O' Dwyer*: Land cover changes in Southern Sweden from the mid-Holocene to present day: Insights for ecosystem service assessments (2019).

110. *Daniel Klingmyr*: Global scale patterns and trends in tropospheric NO2 concentrations (2019).

111. *Marwa Farouk Elkabbany*: Sea Level Rise Vulnerability Assessment for Abu Dhabi, United Arab Emirates (2019).

112. *Jip Jan van Zoonen*: Aspects of Error Quantification and Evaluation in Digital Elevation Models for Glacier Surfaces (2020).

113. *Georgios Efthymiou*: The use of bicycles in a mid-sized city – benefits and obstacles identified using a questionnaire and GIS (2020).

114. *Haruna Olayiwola Jimoh*: Assessment of Urban Sprawl in MOWE/IBAFO Axis of Ogun State using GIS Capabilities (2020).

115. *Nikolaos Barmpas Zachariadis*: Development of an iOS, Augmented Reality for disaster management (2020).

116. *Ida Storm*: ICOS Atmospheric Stations: Spatial Characterization of CO2 Footprint Areas and Evaluating the Uncertainties of Modelled CO2 Concentrations (2020).

117. *Alon Zuta*: Evaluation of water stress mapping methods in vineyards using airborne thermal imaging (2020).

118. *Marcus Eriksson*: Evaluating structural landscape development in the municipality Upplands-Bro, using landscape metrics indices (2020).

119. *Ane Rahbek Vierø*: Connectivity for Cyclists? A Network Analysis of Copenhagen's Bike Lanes (2020).

120. *Cecilia Baggini*: Changes in habitat suitability for three declining Anatidae species in saltmarshes on the Mersey estuary, North-West England (2020).

121. *Bakrad Balabanian*: Transportation and Its Effect on Student Performance (2020).

122. *Ali Al Farid*: Knowledge and Data Driven Approaches for Hydrocarbon Microseepage Characterizations: An Application of Satellite Remote Sensing (2020).

123. *Bartlomiej Kolodziejczyk*: Distribution Modelling of Gene Drive-Modified Mosquitoes and Their Effects on Wild Populations (2020).

124. *Alexis Cazorla*: Decreasing organic nitrogen concentrations in European water bodies - links to organic carbon trends and land cover (2020).

125. *Kharid Mwakoba*: Remote sensing analysis of land cover/use conditions of community-based wildlife conservation areas in Tanzania (2021).

126. *Chinatsu Endo*: Remote Sensing Based Pre-Season Yellow Rust Early Warning in Oromia, Ethiopia (2021).

127. *Berit Mohr*: Using remote sensing and land abandonment as a proxy for long-term human out-migration. A Case Study: Al-Hassakeh Governorate, Syria (2021).

128. *Kanchana Nirmali Bandaranayake*: Considering future precipitation in delineation locations for water storage systems - Case study Sri Lanka (2021).

129. *Emma Bylund*: Dynamics of net primary production and food availability in the aftermath of the 2004 and 2007 desert locust outbreaks in Niger and Yemen (2021).

130. *Shawn Pace*: Urban infrastructure inundation risk from permanent sea-level rise scenarios in London (UK), Bangkok (Thailand) and Mumbai (India): A comparative analysis (2021).

131. *Oskar Evert Johansson*: The hydrodynamic impacts of Estuarine Oyster reefs, and the application of drone technology to this study (2021).

132. *Pritam Kumarsingh*: A Case Study to develop and test GIS/SDSS methods to assess the production capacity of a Cocoa Site in Trinidad and Tobago (2021).

133. *Muhammad Imran Khan*: Property Tax Mapping and Assessment using GIS (2021).

134. *Domna Kanari*: Mining geosocial data from Flickr to explore tourism patterns: The case study of Athens (2021).

135. *Mona Tykesson Klubien*: Livestock-MRSA in Danish pig farms (2021).

136. *Ove Njøten*: Comparing radar satellites. Use of Sentinel-1 leads to an increase in oil spill alerts in Norwegian waters (2021).

137. *Panagiotis Patrinos*: Change of heating fuel consumption patterns produced by the economic crisis in Greece (2021).

138. *Lukasz Langowski*: Assessing the suitability of using Sentinel-1A SAR multi-temporal imagery to detect fallow periods between rice crops (2021).

139. *Jonas Tillman*: Perception accuracy and user acceptance of legend designs for opacity data mapping in GIS (2022).

140. *Gabriela Olekszyk*: ALS (Airborne LIDAR) accuracy: Can potential low data quality of ground points be modelled/detected? Case study of 2016 LIDAR capture over Auckland, New Zealand (2022).

141. *Luke Aspland*: Weights of Evidence Predictive Modelling in Archaeology (2022).

142. *Luís Fareleira Gomes*: The influence of climate, population density, tree species and land cover on fire pattern in mainland Portugal (2022).

143. *Andreas Eriksson*: Mapping Fire Salamander (Salamandra salamandra) Habitat Suitability in Baden-Württemberg with Multi-Temporal Sentinel-1 and Sentinel-2 Imagery (2022).

144. *Lisbet Hougaard Baklid*: Geographical expansion rate of a brown bear population in Fennoscandia and the factors explaining the directional variations (2022).

145. *Victoria Persson*: Mussels in deep water with climate change: Spatial distribution of mussel (Mytilus galloprovincialis) growth offshore in the French Mediterranean with respect to climate change scenario RCP 8.5 Long Term and Integrated Multi-Trophic Aquaculture (IMTA) using Dynamic Energy Budget (DEB) modelling (2022).

146. *Benjamin Bernard Fabien Gérard Borgeais*: Implementing a multi-criteria GIS analysis and predictive modelling to locate Upper Palaeolithic decorated caves in the Périgord noir, France (2022).

147. *Bernat Dorado-Guerrero*: Assessing the impact of post-fire restoration interventions using spectral vegetation indices: A case study in El Bruc, Spain (2022).

148. *Ignatius Gabriel Aloysius Maria Perera*: The Influence of Natural Radon Occurrence on the Severity of the COVID-19 Pandemic in Germany: A Spatial Analysis (2022).

149. *Mark Overton*: An Analysis of Spatially-enabled Mobile Decision Support Systems in a Collaborative Decision-Making Environment (2022).

150. *Viggo Lunde*: Analysing methods for visualizing time-series datasets in open-source web mapping (2022).

151. *Johan Viscarra Hansson*: Distribution Analysis of Impatiens glandulifera in Kronoberg County and a Pest Risk Map for Alvesta Municipality (2022).

152. *Vincenzo Poppiti*: GIS and Tourism: Developing strategies for new touristic flows after the Covid-19 pandemic (2022).

153. *Henrik Hagelin*: Wildfire growth modelling in Sweden - A suitability assessment of available data (2023).

154. *Gabriel Romeo Ferriols Pavico*: Where there is road, there is fire (influence): An exploratory study on the influence of roads in the spatial patterns of Swedish wildfires of 2018 (2023).

155. *Colin Robert Potter*: Using a GIS to enable an economic, land use and energy output comparison between small wind powered turbines and large-scale wind farms: the case of Oslo, Norway (2023).

156. *Krystyna Muszel*: Impact of Sea Surface Temperature and Salinity on Phytoplankton blooms phenology in the North Sea (2023).

157. *Tobias Rydlinge*: Urban tree canopy mapping - an open source deep learning approach (2023).